Available online at www.sciencedirect.com

ScienceDirect

Proceedings of the Combustion Institute 000 (2022) 1–29

Proceedings of the Combustion Institute

www.elsevier.com/locate/proci

How fast can we burn, 2.0

Simone Hochgreb

University of Cambridge, Trumpington St, Cambridge CB2 1PZ, UK

Received 31 January 2022; accepted 21 June 2022
Available online xxx

Abstract

We review the state of the art in measurements and simulations of the behavior of premixed laminar and turbulent flames, subject to differential diffusion, stretch and curvature. The first part of the paper reviews the behavior of premixed laminar flames subject to flow stretch, and how it affects the accuracy of measurements of unstrained laminar flame speeds in stretched and spherically propagating flames. We then examine how flow field stretch and differential diffusion interact with flame propagation, promoting or suppressing the onset of thermodiffusive instabilities. Secondly, we survey the methodology for and results of measurements of turbulent flame speeds in the light of theory, and identify issues of consistency in the definition of mean flame speeds, and their corresponding mean areas. Data for methane at a single operating condition are compared for a range of turbulent conditions, showing that fundamental issues that have yet to be resolved for Bunsen and spherically propagating flames. Finally, we consider how the laminar flame scale response of flames to flow perturbations interacting with differential diffusion leads to very different outcomes to the overall sensitivity of the burning rate to turbulence, according to numerical simulations (DNS). The paper concludes with opportunities for future measurements and model development, including the perennial recommendation for robust archival databases of experimental and DNS results for future testing of models.

Keywords: Premixed flames; Turbulent flames; Lewis numbers; Measurement

1. Introduction

In 1992, Derek Bradley gave a lecture at the International Symposium, entitled 'How Fast Can We Burn' [1], in which he attempted to summarize what was then known about the role of turbulence on the burning rate of mixtures, and how molecular diffusion played a role in the microstructure of turbulent flames. The present review was inspired by the same need to understand from the bottom up both how flow fields, reaction and diffusion interact to affect laminar flames, and how these effects go on to generate somewhat peculiar behavior observed in turbulent flames. The task of measurement and validation of models for a variety of mixtures with different thermo-diffusive properties has become particularly important as we are transitioning from carbon-based fuels, for which molecular diffusivity and different reactivity regimes may be quite different from usual hydrocarbons.

E-mail addresses: simone.hochgreb@eng.cam.ac.uk, sh372@cam.ac.uk

https://doi.org/10.1016/j.proci.2022.06.029

The evolution of premixed laminar and turbulent premixed and stratified combustion is relevant to a large class of situations converting chemical to thermal energy. Turbulent flows for combustion devices are generally designed to maximize entrainment and promote flame stabilization, producing high rates of burning per unit volume. Large turbulent scales originating from the incoming geometry direct the flow, for example by generating swirl, shear or tumble, which control entrainment and often couple with acoustics to generate combustion instabilities. Heat release takes place at the flame scales, governed by the rate of mixing and reaction, which are in general enhanced by turbulent fluctuations. The overall reaction rate per unit volume is ultimately governed by the extent to which turbulent velocity fluctuations increase mixing of products and reactants in such a way as to enhance the rate of reaction. Velocity and scalar fluctuations are coupled to the process of combustion, demanding predictions that must span a wide range of spatial and time scales for accurate predictions, as discussed in books [2–4] and reviews [5–9] over the past decade.

Experiments and models to represent the behavior of premixed flames have co-evolved throughout history since the first experiments in laminar flames by Mallard and Le Chatelier and Lewis and von Elbe [10,11] and the earliest experiments of Damköhler in turbulent flames [12]. The original findings and theories continue to form the backbone of our thinking on the subject, but increasingly sophisticated methods have become available in the form of optical diagnostics, theoretical understanding, and sheer computational power for detailed simulations, allowing a much closer exploration of the underlying physical phenomena.

Understanding of the behavior of laminar flames has advanced to a very high level of fidelity for mixtures for which detailed and verified chemical kinetic models exist. Direct numerical simulations (DNS) of the steady and unsteady behavior of laminar flames abound [13–16]. However, not all predictions have been or can be experimentally verified or verifiable. In some cases, it is difficult to experimentally recreate an idealized simulation condition. More generally, simulations are relatively inexpensive relatively to experiments, so the former are significantly more abundant. Yet it is important to continue to test models against experiments. Even though direct numerical simulations with well established chemical kinetic models are trusted, it is not uncommon that previously neglected phenomena are found to be relevant once comparison with experiments is made. Further, as experimental conditions march to still unexplored regions, extrapolations of chemical kinetic models may not be entirely trustworthy.

DNS for turbulent flames has evolved to be able to simulate increasingly complex geometric, flow and chemistry models, including laboratory scale jet flames [17], bluff-body stabilized flames [18] and swirling flows [19]. However valuable, such simulations are typically very expensive, and alternative methods continue to be developed to lower the computational cost for practical simulations.

The current practice in simulation and validation of turbulent premixed flame models involves conducting computational fluid dynamics (CFD) simulations via either Reynolds-averaged Navier-Stokes (RANS/uRANS) or increasingly, with higher fidelity, by large eddy simulations (LES). Embedded in these simulations are the closure or sub-grid models for the expected behavior of the reaction rate or flame speeds subject to the action of turbulence in the unresolved scales. A number of excellent recent reviews have covered the evolution and validation of ever more sophisticated models, almost invariably based on closures generated by DNS [3,4,6,7,20,21]. Simulations based on these models attempt to reproduce the growing experimental database for steady and unsteady flame phenomena, new fuels and higher turbulence operating conditions [22–24]. The expansion of such experimental databases into new directions beyond premixed and non-premixed flames, including stratification, sprays and the behavior of flames with respect to extinction and reignition is very important, and will doubtless continue.

In this review, we take a much narrower lens to focus on how well the science is progressing in producing coupled experiments and models in the quest for understanding of a class of well-controlled experiments for laminar and turbulent premixed flames. In particular, we focus on how experiments and models designed for extracting the laminar and turbulent flame speeds have fared, and how they have informed the understanding of the science. Along the way, we try to identify gaps in the experimental database, as well as areas where the understanding of the phenomena is incomplete.

The purpose in the present review is to draw a (more or less) direct line between the physics of premixed flames under the role of differential diffusion and stretch (associated with tangential stretch and curvature), the onset of instabilities, and on to the physics and measurement of turbulent flames.

The paper is organised as follows. In the first part, we review laminar flame speeds: governing equations, methods of measurements, and the current state of understanding and prediction of these measurements. In the second part, we consider ideal turbulent premixed flames: averaged governing equations, and selected, well-controlled experiments on burning rates. We then assess the state of understanding for these measurements and their interpretation. Finally, we turn our attention to the role of differential diffusion in the behavior of turbulent flames, and the relative paucity of well controlled experiments with sufficiently de-

Please cite this article as: S. Hochgreb, How fast can we burn, 2.0, Proceedings of the Combustion Institute, https://doi.org/10.1016/j.proci.2022.06.029

tailed measurements. The paper concludes with a series of considerations and recommendations for future work.

2. General governing equations

In order to make the subsequent discussions easier, we start from a summary of the governing equations for laminar flows for mass, species and low Mach number momentum conservation, along with the ideal gas equation. The mass and momentum conservation equations are common to fluid mechanics, so the coupling with species and energy conservation equation deserve special attention in combustion. The conservation equation for density ρ, velocity $\mathbf{u}$, pressure p, N_s species mass fraction, Y_i and enthalpy h are given as [2,25]:

$$\frac{\partial \rho}{\partial t} + \nabla \cdot (\rho \mathbf{u}) = 0 \tag{1}$$

$$\frac{\partial}{\partial t}(\rho \mathbf{u}) + \nabla \cdot (\rho \mathbf{u}\mathbf{u}) = -\nabla p + \nabla \cdot \mathcal{T} + \rho \mathbf{g} \tag{2}$$

$$\frac{\partial}{\partial t}(\rho Y_i) + \nabla \cdot (\rho \mathbf{u} Y_i) = \nabla \cdot \left(\frac{1}{\mathrm{Le}_i} \frac{\lambda}{c_p} \nabla Y_i \right) + \omega_i \tag{3}$$

$$\frac{\partial}{\partial t}(\rho h) + \nabla \cdot (\rho \mathbf{u} h) = \nabla \cdot \left(\frac{\lambda}{c_p} \left(\nabla h + \sum_{i=1}^{N_s} \left(\frac{1}{\mathrm{Le}_i} - 1 \right) h_i \nabla Y_i \right) \right) \tag{4}$$

where $\mathcal{T}$ is the viscous stress tensor, $\mathbf{g}$ is gravity (neglected in what follows), the Lewis number $\mathrm{Le}_i = \frac{\alpha}{\mathcal{D}_i}$ is the ratio of the bulk thermal diffusivity, $\alpha = \lambda/(\rho c_p)$, to the species diffusivity in the bulk mixture, ω_i is the reaction rate per unit volume of species i, and the properties λ and c_p are the thermal conductivity and specific heat of the bulk mixture. The enthalpy $h(T, \mathbf{Y}) = h_s(T, \mathbf{Y}) + \sum_{i=1}^{N_s} h_{i,\mathrm{ref}} Y_i$ is the sum of the sensible and chemical enthalpy for the sum of all species in the vector $\mathbf{Y} = [Y_1, \ldots Y_i, \ldots, Y_{N_s}]$, so that the change in species is coupled to the energy equation, and can be expressed as a source term to the energy equation. The last term in the energy equation is usually neglected in mixtures with near unity Lewis number. This formulation is not atomically conservative, but often sufficiently accurate for flame calculations, with the benefit of simplicity. Soret (temperature driven) species diffusion is neglected here, although in the case of very light or heavy molecules, they should be included for accuracy.

In the discussion of premixed flames, it is useful to consider the conservation equation for a progress of reaction variable, c, which is usually a linear combination of scalars, often either reactants or products. Its balance can be derived from the conservation equations for the selected scalars, and is expressed in a similar manner as the species or energy balance,

$$\rho \frac{\partial c}{\partial t} + \rho \mathbf{u} \cdot \nabla c = \nabla \cdot (\rho \mathcal{D}_c \nabla c) + \dot{\omega}_c \tag{5}$$

where the diffusion coefficient $\mathcal{D}_c$ becomes a corresponding weighted sum of the diffusivity of the scalars chosen.

A displacement speed s_d is a measureable quantity defined as the normal velocity at a contour $c = c^*$ [26], as is its density weighted counterpart, $\tilde{s}_d$,

$$s_d = \frac{1}{|\nabla c|} \frac{\mathrm{D}c}{\mathrm{D}t} = \frac{1}{\rho |\nabla c|} [\nabla \cdot (\rho \mathcal{D}_c \nabla c) + \dot{\omega}_c] \tag{6}$$

$$\tilde{s}_d = \frac{\rho}{\rho_u} s_d \tag{7}$$

where the subscripts u and b correspond to unburned and burned values of the property, and the total derivative operator is $\frac{\mathrm{D}}{\mathrm{D}t}(\cdot) = \frac{\partial}{\partial t}(\cdot) + \mathbf{u} \cdot \nabla(\cdot)$.

Finally, a consumption speed can be determined based on integration of Eq. (5) averaged over a volume in the direction of flame propagation, here chosen to point into the reactants, $\mathbf{n} = -\frac{\nabla c}{|\nabla c|}$:

$$s_c = \int_{-\infty}^{+\infty} \frac{\dot{\omega}_c}{\rho |\nabla c|} \mathbf{n} \cdot \mathrm{d}\mathbf{s} \tag{8}$$

and $\mathbf{s}$ is the coordinate vector across the flame.

3. Measurements and uncertainties in the determination of laminar flame speeds

3.1. Measurements of laminar flame speeds

Accurate measurements of laminar flame speeds are necessary for the understanding of a very large range of phenomena in combustion. These are required both directly, as a key parameter in the design of burners, as well as indirectly, since chemical kinetic models used for turbulent combustion are frequently validated against measurements of laminar flame speeds. In this section, we take a brief look at the state of understanding and agreement between models and experiments of laminar flame speeds. The laminar flame speed is usually defined as the displacement speed of an isotherm associated with the leading edge of the flame, Eq. (7). Its value depends not only on the composition of the fresh mixture, but also on the flow field within which it is propagating. In particular, it is affected by stretch, or the rate of divergence of the streamlines in the field. The usual term laminar flame speed refers to the theoretical value of the *unstretched*, or free laminar flame speed, s_L^0. The definition corresponds to

Please cite this article as: S. Hochgreb, How fast can we burn, 2.0, Proceedings of the Combustion Institute, https://doi.org/10.1016/j.proci.2022.06.029

the displacement velocity of the reactant end, s_d, Eq. (7), for the case of a planar flame propagating in stretch-free flow. Under these conditions, its value is equal to the consumption speed, s_c, Eq. (8).

An excellent review of measurement techniques for laminar flame speeds was provided by Egolfopoulos et al. [27], and a comprehensive compilation of measurements of fuel/air mixtures and their comparisons with the most experimental models has been recently provided by Konnov et al. [28]. The work in [27] focuses on how to most accurately extract information on the unstretched laminar flame speed as a reference, as well as on measurements of the profile of species in low-pressure stabilized flames for purposes of developing chemical mechanisms. In [28], the purpose is to investigate the state of agreement between model and experiments for a wide range of air-fuel mixtures. The latter review does not include comparisons for all possible fuels (olefins, aromatics and biofuels, for example), or multicomponent fuels. However, it offers a wealth of well curated information on the state of the art and comparisons with results of simulations using well established chemical kinetic models. The state space of pressures and temperatures covered in the review is available for C1-C10 aliphatic hydrocarbons and alcohols (and DME) mixtures with air is shown in Fig. 1. Other comprehensive studies include the work of Farrell et al. [29], who measured the burning rate of a variety of hydrocarbons using the spherically expanding flame method for pressures around 3 bar and 450 K, the historical work of Bradley in spherically propagating flames [30–33], and that of Law and Egolfopoulos in stagnation and spherical flames [27,34–37]. The abundance (and in some areas, absence) of measurements in the Konnov review is representative of the existing data in the literature for selected fuels. There are plentiful measurements at ambient conditions, but a much more scattered and smaller set of data at high temperatures and pressures. Measurements are desirable both for mixtures with air and fuel, as well as with the respective high temperature burned gases, so as to simulate exhaust gas recirculation (in engines) and premixing with recirculated products in gas turbines. The difficulties in covering the relevant state space needed for applications at high pressure and temperature are well known, as the costs of operation and complexity increase with higher pressure and temperature. Validation at high temperature and pressure conditions with dilution by burned gases is particularly hard to generate and may continue to be bridged using models.

Fig. 2 shows a summary of all measurements considered in the review by Konnov et al. [28] at all temperatures and pressures, here excluding hydrogen, which has a much wider range of flame speeds. There are not many data points for temperatures beyond 450 K even for simple mixtures. Flame speeds are confined to a range below about 60 cm/s near ambient conditions for most hydrocarbons and alcohols. Laminar flame speed dependence is usually scaled to higher pressures and temperatures using a power law, with a positive exponent of the order of 1.5–2.0 for temperature, and of negative order 0.2–0.5 for pressure, for most hydrocarbons. However, only certain fuels have been investigated over a wide enough range to provide sufficient information. For very well studied fuels, such as methane, n-heptane, i-octane and dodecane, uncertainties and disparities with available chemical kinetic models are of the order of 10–20% at ambient conditions. Increasing disparities of factors of two or higher appear at higher temperatures and pressures beyond 5 bar, where there are fewer data points. Considering the importance of these fuel mixtures for practical purposes, it is actually surprising that we still do not have better information and models to be used. The shortcoming is one of the reasons why direct experimentation and comparison with models in actual combustors is often needed. Inaccuracies in model fundamentals are often practically corrected by semi-empirical adjustments for engineering purposes, while the science catches up with technology.

Fig. 3 shows a sample of the relatively scarce high pressure measurements of fuels used as surrogates for the gasoline reference fuels, i-octane (triangles) and n-heptane (circles), for pressures up to 25 bar, along with predictions using the mechanism of [38]. The measurements show that pressure decreases the laminar flame speed of the two fuels, and that the proposed chemical kinetic model adequately captures the behaviour. The right- and left- pointing open triangles represent data acquired from pressure data (right) and schlieren (left), demonstrating the quantitative differences obtained in measurements extracted in the same facility using different methods. All measurements above 5 bar have been acquired from spherically propagating flames, and the ones at the highest pressures typically rely on pressure data only. The extraction of unstretched laminar flame speeds from spherically expanding flames using either images or pressure rise is subject to inherent errors associated with the effect of stretch, and these are discussed in the following section.

Hydrogen (H_2), ammonia (NH_3) and blends with methane have received significant attention as potential low-carbon replacement fuels [39,40]. A number of studies throughout history, and a recent spate of experiments and reviews have created a solid database for laminar flame speed measurements for hydrogen and blends with hydrocarbons over a wide range of pressures, equivalence ratio and dilution conditions, and a modest range of temperatures [34,37,41–46]. Hydrogen is a most unusual fuel, as its very high diffusivity and reactiv-

Please cite this article as: S. Hochgreb, How fast can we burn, 2.0, Proceedings of the Combustion Institute, https://doi.org/10.1016/j.proci.2022.06.029

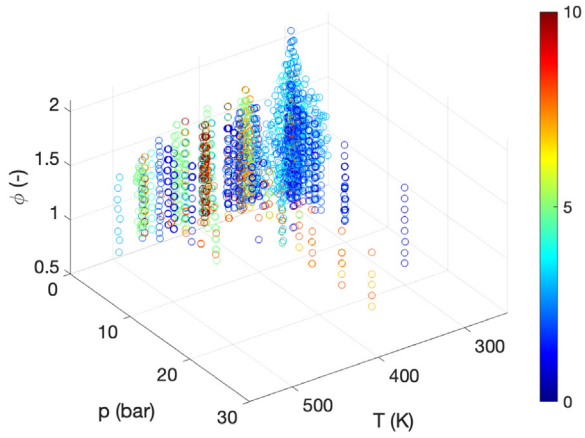

Fig. 1. State space (pressure, temperature and equivalence ratios) of measurements compiled in the laminar flame speed review by Konnov et al. [28] for mixtures of 14 fuels and air (C1-C10 aliphatic hydrocarbons, alcohols and DME). Open circles are hydrocarbons, squares are alcohols and DME; colorbar represents the number of carbons in the molecule.

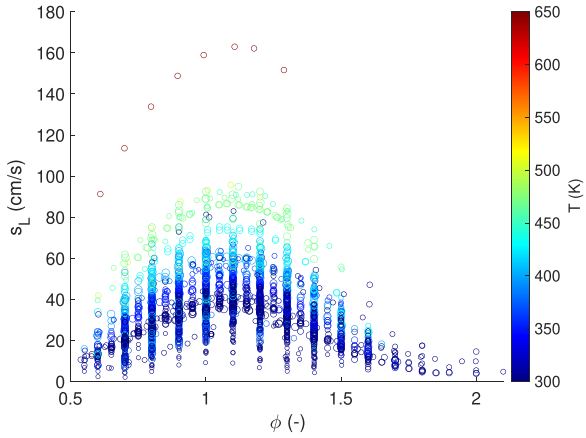

Fig. 2. Measured laminar flame speeds in the same mixtures considered in Fig. 1 as a function of equivalence ratio and temperature (for all pressures). Symbol sizes are scaled according to number of carbons in the molecule, and the colorbar denotes temperature.

ity lead to peak laminar flame speeds of 300 cm/s in ambient air at an equivalence ratio around 1.8, with a very steep slope from the lean flammability limit around 0.30. Konnov's review [28] and recent studies [37,42,46] suggest that good agreement (< 20%) can be found between one-dimensional flame models of laminar flame speeds and experiments at the conditions measured over most of the range of equivalence ratio (except near the very lean end), as well as in mixtures with methane, carbon monoxide, and well-studied hydrocarbons. In the case of ammonia, there has been a recent flurry of activity in acquiring measurements of mixtures with syngas, hydrogen, and methane, over a range of conditions and pressures, leading model adjustments [47–53]. As ever, both experimental results and models are under continued revision as more accurate experimental results and models become available.

3.2. *Laminar flame speed measurements and the role of stretch*

In the previous subsection, we have taken a broad overview to the comparison of the unstretched, adiabatic laminar flame speed, which is a reference quantity for many models. Yet it is remarkably difficult to produce such a flame in practice. The most popular methods for extracting laminar flame speeds are: (a) steady counterflow flow flames (CFF), (b) unsteady, spherically expanding flames (SEF), (c) steady heat flux method (HF). All three methods have inherent advantages of symmetry and thus one-dimensionality, a reason for

Please cite this article as: S. Hochgreb, How fast can we burn, 2.0, Proceedings of the Combustion Institute, https://doi.org/10.1016/j.proci.2022.06.029

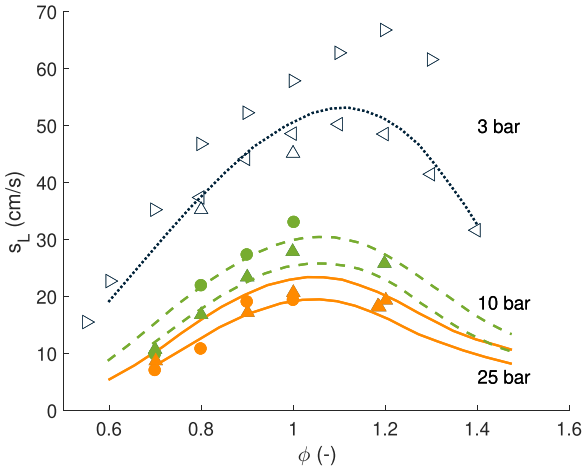

Fig. 3. Measured laminar flame speeds for n-heptane (circles) and i-octane (triangles) and respective modelling (lines) for three pressures in the same mixtures considered in Fig. 1 as a function of equivalence ratio and temperature (for all pressures). The right and left triangles for the 3 bar measurements represent measurements by [29] in spherically propagating flames using pressure data (right triangles) and schlieren visual measurements (left triangles). Data from [29,31,54], modelling by [28] using the mechanisms by [38].

their superiority relatively to *e.g.* Bunsen stabilised or other methods. The detailed advantages of the different methods are discussed in detail in [27,28], but in general one can say that the SEF method offers the ability to investigate higher pressures and temperatures (the latter often through adiabatic heating due to compression during propagation), whereas the steady flame methods offer the ability to explore flame structure using optical diagnostics. The heat flux method produces flames that are not affected by aerodynamic stretch, but requires attention to the temperature distribution around the burner in order to extract the adiabatic value. In this section, we review the two most used methods, CFF and SEF, their uncertainties and dependence on assumptions and the current understanding of best practices. The measurement methods and their accuracy are closely connected to the role of flow stretch on the flame, how it affects the measured displacement speeds, and ultimately how measurements can be extrapolated to those of unstretched flames for comparison between results of different methods.

Stretch is usually defined as the rate of change of a local isocontour area element associated with the flame, dA, which moves with absolute velocity $\mathbf{s}_f$ in a field of velocity $\mathbf{u}$ as [55]:

$$K = \frac{1}{A}\frac{\mathrm{d}A}{dt} = \nabla_t \cdot \mathbf{u} + s_d \nabla \cdot \mathbf{n} \tag{9}$$

where $K_t = \nabla_t \cdot \mathbf{u}$ is the divergence of flow velocity in the tangential direction, along the isosurface itself, and $s_d = (\mathbf{s}_f - \mathbf{u}) \cdot \mathbf{n}$ is the surface normal displacement speed relatively to the flow velocity $\mathbf{u}$, so that second term on the RHS represents the stretch associated with curvature of the isosurface, $\kappa_c = \nabla \cdot \mathbf{n}$. In the case of steady planar CFFs, we have $K = K_t = \nabla_t \cdot \mathbf{u}$. For SEFs, the total stretch is equal to $K = \frac{2}{R}\frac{dR}{dt}$, where R is the flame radius, and the initially high positive stretch decreases as the radius increases during flame expansion.

3.3. Counterflow laminar flame (CFF) measurements and modeling

The CFF method, developed by Law and coworkers as a flexible technique, relies on the measurement of the flow field speed along the centreline of an opposed, premixed, axisymmetric flow in a twin or stagnation flame arrangement [36,56–59]. The flow speed is measured throughout the centerline of the flame, and the minimum velocity, s_{ref}, upstream of the flame acceleration is associated with a characteristic strain rate given by the gradient of velocity in the radial direction, $\nabla_t \cdot \mathbf{u}$.

Models for the effect of velocity gradients in stabilised flames such as CFFs were originally derived by Karlovitz et al. [60], and a concise discussion of the background is available in [61]. The simplest model of the effect of stretch leads to a linear decrease in flame speed [36,60–63]:

$$s_{u,\mathrm{ref}} = s_u^0 - \mathcal{L}K \tag{10}$$

where $\mathcal{L}$ is a proportionality constant called the Markstein length scale, and $s_u^0 = s_L^0$. According to this approximation, measurements of the local flame speed at a given stretch can be linearly extrapolated to zero stretch to obtain the unstretched laminar flame speed.

Matalon, Law and colleagues [63–65] derived an expression for the ratio of the stretched reference flame speeds as a function of stretch in CFFs. Here

Please cite this article as: S. Hochgreb, How fast can we burn, 2.0, Proceedings of the Combustion Institute, https://doi.org/10.1016/j.proci.2022.06.029

we present the expression for the ratio in a slightly different form, in order to separate the terms that depend either only on the unstretched expansion ratio, $\sigma = \rho_u/\rho_b$, from those that depend on both expansion ratio and the Lewis number [63,66]:

$$\frac{s_{u,\mathrm{ref}}}{s_L^0} = 1 - \mathcal{M}\mathrm{Ka} \tag{11}$$

$$\mathcal{M} = (\mathcal{M}_\sigma + \mathcal{M}_\mathrm{D}) \tag{12}$$

$$\mathcal{M}_\sigma = \frac{\sigma \ln \sigma}{\sigma - 1} - 1 - \ln(\sigma - 1) + \ln(\mathrm{Ka}) \tag{13}$$

$$\mathcal{M}_\mathrm{D} = \frac{(\mathrm{Le} - 1)}{\sigma - 1}\frac{Ze}{2} I_\sigma \tag{14}$$

$$I_\sigma = \int_1^\sigma \ln \frac{\xi}{1 - \xi}\, d\xi \tag{15}$$

where a Karlovitz number is a non-dimensional product of stretch rate and unstretched flame residence time, $\mathrm{Ka} = K\tau_f$, $\mathrm{Ze} = \frac{T_a}{T_b}(\sigma - 1)$ is a Zeldovich number for an activation temperature T_a, $\mathcal{M}_\sigma$ is a Markstein number associated with the expansion of the gas, and $\mathcal{M}_\mathrm{D}$ is associated with the Lewis number of the deficient species. Additional terms appear if the thermal conductivity is assumed to also depend on temperature. In the literature, the set of equations is often referred to as the non-linear (NL) extrapolation, as $\mathcal{M}_\sigma$ itself depends on Ka.

The physical meaning of these equations is illustrated in Fig. 4. Mass conservation means that there is a net outflow proportional to positive stretch, which depends on the density profile within the preheat zone, leading to the first term in the equation, $\mathcal{M}_\sigma$, which is positive for typical values of σ. For $\mathrm{Le} = 1$ of the deficient species, the flame moves to accommodate a reduced mass flux resulting from higher stretch, but the structure of the flame is unchanged. For non-unity Lewis number, $\mathcal{M}_\mathrm{D}$ depends on the Lewis number of the deficient species. For lean mixtures, if the diffusivity of fuel is higher than that of heat ($\mathrm{Le}_F < 1$), stretch leads to higher diffusion of fuel into the reacting zone, thus increasing the burning rate. For $\mathrm{Le}_F > 1$, the reverse is true, and the corresponding burning rate decreases, as reflected in the sign of the second term, $\mathcal{M}_\mathrm{D}$. The rationale is flipped for the rich range, in which oxygen is the limiting species. The specific details also depend to some extent on the chemistry of the limiting reactants, but the overall behavior is reasonably well captured by the theory once the correct dependence of temperature for density and and conductivity is represented.

The terms associated with σ in $\mathcal{M}_\sigma$ take negative values between 0.2 to 0.5 for typical values of σ. For moderate Ka, this means that the slope of

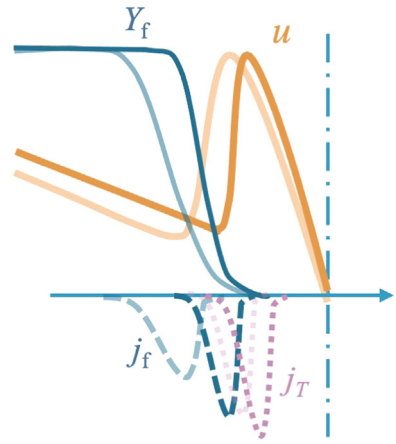

Fig. 4. Diagram of centerline velocity (u, solid orange), fuel mass fraction (Y_f, solid blue), fuel diffusion flux (j_f, dashed blue) and heat flux (j_T, dotted magenta) for a CFF, for low (light) and high (dark) stretch for non-unity Lewis number. (For interpretation of the references to color in this figure legend, the reader is referred to the web version of this article.)

$\frac{s_{u,\mathrm{ref}}}{s_L^0}$ with Ka depends on the value of $\mathcal{M}_\mathrm{D}$, which is directly proportional to $(\mathrm{Le} - 1)$ of the deficient species. For Le near unity, the slope approaches the value of $\mathcal{M}_\sigma$, near zero stretch, as the change in heat flux is balanced by that of limiting species. In the lean range, the deficient species is typically the fuel, and in the rich range, oxidizer. For lean dodecane mixtures, $\mathrm{Le} \approx 4.4$, the slope is typically negative with Ka. Conversely, for lean hydrogen flames, with $\mathrm{Le} \approx 0.3$ the slope becomes positive.

The results presented in the extensive work by Law and coworkers [64,65,67] show that non-linear fits to experimental data for the total Markstein number $\mathcal{M} = \mathcal{M}_\sigma + \mathcal{M}_\mathrm{D}$ using Eq. (12) and s_L^0 can yield values of the unstretched laminar flame speeds that agree within 10–20% of values obtained from other methods. Alternatively, comparisons of model and experiments at any Ka can be made directly using chemical-diffusive models of strained flames, with no attempt to extrapolate values to zero stretch, when such models are available.

Many models for turbulent flames are based on the idea of flamelets under stretch via reduced chemical models or tabulation, where the flame structure and burning rate includes the effect of chemistry, differential diffusion and stretch as control parameters in look-up tables [25,68–73].

The formulation of De Goey et al. [25,74,75] on the effect of differential diffusion and stretch is particularly clearly presented, as it lends itself readily for integration with tabulation methods for turbulent combustion computations of premixed and stratified mixtures, as reviewed in [70,76]. The results are compared to the limit theoretical re-

Please cite this article as: S. Hochgreb, How fast can we burn, 2.0, Proceedings of the Combustion Institute, https://doi.org/10.1016/j.proci.2022.06.029

sults using different approximations [61,77]. The formulation considers a mass-based rather than area-based stretch along a stretched flamelet. The method is the basis of the flame generated manifold (FGM) method [74], which, along with other tabulation methods, has been successful in making predictions for premixed and partially premixed flames with realistic chemistry and stretch effects.

Fig. 5 shows how different approximations are able to account for the fractional decrease in burning rate per unit area relative to that of the unstretched flame, m_b/m_b^0, by comparison to detailed numerical simulations. In the case of a lean flame (top), all approximations which take into account the effect of stretch on the burned gas temperatures give good approximations for the effect of stretch on flames. However, for the case of a rich flame (bottom), the only approximations that work are those that account for detailed species and temperatures (solid line), including at least the correct equilibrium temperatures (green line).

The inclusion of differential diffusion in turbulent flame simulations (and of course appropriate chemistry manifold) is particularly important in the case of mixtures with limiting Lewis numbers very different than unity. Examples exist for flames with hydrogen and methane [72], and where significant stratification occurs between rich and lean mixtures [78]. The effect of stretch in turbulent flame calculations has also been explored in [68,73] using correlated control variables. The latter are particularly important at lower values of turbulence and at lower temperatures. Recent work has demonstrated that the contributions of curvature and tangential stretch are different [79,80]. This means that turbulent combustion models may need to be further specialized to integrate the prevalence of curvature relatively to tangential stretch, particularly for Lewis numbers far from unity. The next section reviews laminar flame measurements where stretch appears from the time-dependent curvature of the flame.

3.4. Spherically expanding flame (SEF) measurements and modeling

The SEF method for stretched flame was originally introduced by [81]. In SEFs, the main observable is the propagation speed of the burned flame front $s_f = \frac{dR}{dt}$. The density-weighted flame front velocity relatively to the unburned gases, $\tilde{s}_u$ or to the burned gases, $\tilde{s}_b$, is given by:

$$\tilde{s}_u = \frac{\rho_b}{\rho_u}(s_f - u_u) \tag{16}$$

$$\tilde{s}_b = \frac{\rho_b}{\rho_u}(s_f - u_b) \tag{17}$$

The burned gases remain stationary as the flame passes, so that $u_b \approx 0$, and

$$\tilde{s}_b = \frac{\rho_b}{\rho_u}\frac{dR}{dt} \tag{18}$$

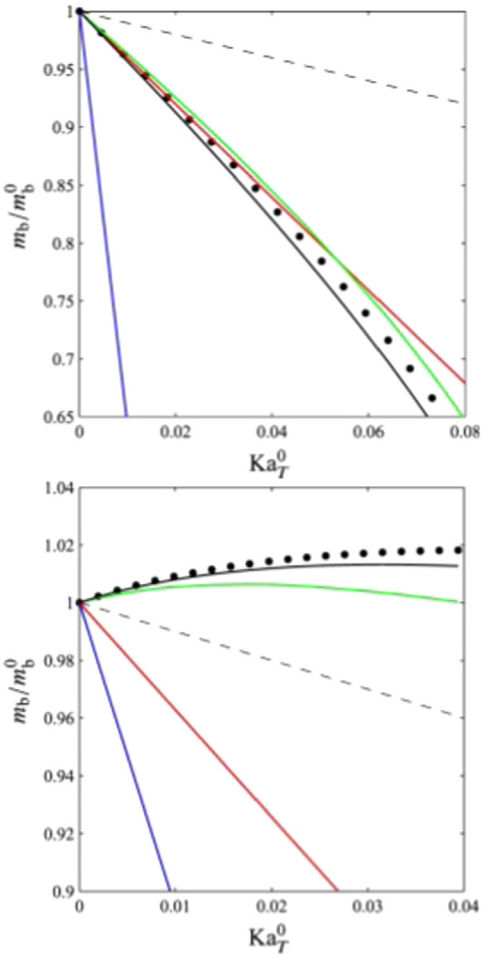

Fig. 5. Normalized mass burning rate of stretched propane-air flames as a function of Ka_T^0. Top: Lean mixture ($\phi = 0.6$). Bottom: Rich mixture ($\phi = 1.5$). Spherical markers: numerical simulations. Solid black line: simplified calculation of integral, based on numerical values for temperature and species. Dashed black line: $1 - Ka_T^0$. Solid green line: $1 - Ka_T^0 + \frac{Ze}{2}\frac{T_b - T_u}{T_b^{ad} - T_u}$, with values of T_b from numerical simulation. Red line: $1 - Ka_T^0 + \frac{Ze}{2}(\frac{Ka_D^0}{Le_D} - Ka_T^0)$. Blue line: asymptotic value using $\mathcal{M}$ calculated in the burned gases. Ka_T^0 and Ka_D^0 are non-dimensional integral Karlovitz numbers based on temperature or diffusive species weighting profile weighting, obtained from unstretched flame profiles. The reader is directed to the original paper for detailed definitions. Reprinted from [25]. (For interpretation of the references to color in this figure legend, the reader is referred to the web version of this article.)

Measurements of $R(t)$, typically via schlieren images, can therefore be used to extract $\tilde{s}_b$, with suitable assumptions for the density ratio $\sigma = \rho_u/\rho_b$. However, note that whereas u_b is zero owing to symmetry, u_u is actually positive, as the gas expands and pushes the fresh mixture away. There-

Please cite this article as: S. Hochgreb, How fast can we burn, 2.0, Proceedings of the Combustion Institute, https://doi.org/10.1016/j.proci.2022.06.029

fore, $s_u = s_L$ cannot be obtained directly unless u_u is measured. Second, the flame is expanding, so that the area stretch is $K = \frac{2}{R}\frac{dR}{dt}$. Models must therefore be developed to take into account the effect of stretch on the flame, and to extrapolate results to zero stretch. Finally, we note that the value of K decreases as the radius increases, so that the effect of stretch is larger where the radius is small.

A pair of elegant papers by Giannakoupoulos et al. [15,66] combined DNS and theory for SEF propagation, distinguishing the differences between displacement and consumption speeds. The density weighted displacement speed at any arbitrary isotherm $\tilde{s}_d$ can be obtained,

$$\left(\frac{\tilde{s}_d}{s_L^0}\right) = 1 - \mathcal{M}\mathrm{Ka} \tag{19}$$

The value $\mathcal{M}$ in this formulation is the same as (12) in the limit of fixed thermal conductivity (additional terms arise in Ka for temperature-dependent properties, see [66]). The value of the apparent slope of the displacement speed to strain, *i.e.* the respective Markstein number, is usually calculated relative to the unburned isotherm. However, the value of the Markstein number was shown to be extremely sensitive to the particular isotherm chosen for its definition towards the unburned edge, yet its value converges to a single well-defined value near zero at the burned gases. Experimental measurement of such displacement speeds near the burned gases is difficult, however, but should be encouraged for validation purposes. The sensitivity reflects the role of the variable density and thermal conductivity within the thermal layer of the flame, as the displacement speed depends on the choice of isotherm. Therefore, one should be extremely careful about using or extrapolating values obtained for $\mathcal{M}$ at different isotherms. The cited work shows how the asymptotic theory using the Ka-dependent Markstein number and direct numerical simulations agree very well [15,66] once a careful dependence on the isotherm is taken.

An asymptotic solution to the problem laminar SEFs by Frankel et al. [82,83] for the velocity relative to the burned gas, for flames of large radius, large activation energy, propagating in steady state is often used:

$$\left(\frac{\tilde{s}_b}{\tilde{s}_b^0}\right)^2 \ln\left(\frac{\tilde{s}_b}{\tilde{s}_b^0}\right)^2 = -2\sigma\mathcal{M}_b\mathrm{Ka_b} = -2\frac{\mathcal{L}_b}{\tilde{s}_b^0}K \tag{20}$$

where the value of $\mathcal{L}_b$ and $\tilde{s}_b^0$ are usually obtained from experiments using a fitting procedure. A number of investigators have applied this non-linear technique to both extract the parameters $\tilde{s}_b^0$, $\mathcal{M}_e$ for a given mixture [84–86] from the existing $\tilde{s}_b(R(t))$ datasets. The extracted parameters are then further compared to numerical and theoretical results at zero strain obtained from other types of experiments.

The past decade has led to a number of outstanding joint efforts from experimentalists and modellers using a combination of 1D and 2D numerical simulations to both unravel the effect of stretch on CFFs and SEFs, and to find a consistent and coherent way to either extrapolate the results zero strain, or to directly compare simulations to experiments. An interesting exercise investigating the soundness of the extrapolation techniques was performed by [85] for hydrogen and heptane datasets in SEFs, as shown in Fig. 6. The red/green circles show the experiments, the black dots show the DNS displacement speeds, and the blue dots the consumption speeds. For n-heptane, no experiments are shown, only simulations. The numerical results show a negative slope with stretch for values of ϕ from 0.7 to 1.3, after which the values become positive. The extrapolations are extracted for a range of values of $\tilde{s}_b(K)$ near which the behavior is linear. For both linear and non-linear extrapolations, the zero-stretch values are within 20% of the calculated unstretched value. For hydrogen, the behavior with equivalence ratio is reversed, as expected from the low value of Le. Measured and calculated weighted displacement speeds have large positive slopes with stretch for ϕ from 0.4 to around stoichiometric, and negative slopes for ϕ above stoichiometric. There is good agreement of the measured displacement speeds (red/green) with the full numerical simulations (black dots). However, the fitted and extrapolated values in the lean range yield significant discrepancies of factors of up to 1.8 compared to the calculated limit values.

Recent developments by INSA-Rouen [14,87] have been implemented to directly measure an average consumption speed for flame mixtures in SEFs, validating the approach for methane mixtures. The approach is based on the integral balance of a progress of reaction variable, yielding:

$$\langle s_c \rangle = \frac{dR}{dt} - \frac{R_0^3 - R^3}{3R_0^3}\frac{1}{\rho_u}\frac{d\rho_u}{dt} \tag{21}$$

where R_0 is the equivalent radius for the vessel volume. Here the second term of the equation involving ρ_u is evaluated using sub-pixel correlative PIV. The method bypasses the required assumption for a burned gas density in Eq. (17) in favour of a direct measurement, which agrees very well with predictions under stoichiometric conditions, as shown in Fig. 7. The agreement is less favorable for lean conditions (not shown), as the velocity is determined by subtraction of two large numbers. We also observe that the value of the consumption flame speed (green symbols) is much less sensitive to stretch compared to the displacement speeds, as expected from the simulations.

3.5. Flame instabilities

Laminar flames can develop instabilities under the action of hydrodynamic and thermo-diffusive instabilities. These arise under conditions in which

Please cite this article as: S. Hochgreb, How fast can we burn, 2.0, Proceedings of the Combustion Institute, https://doi.org/10.1016/j.proci.2022.06.029

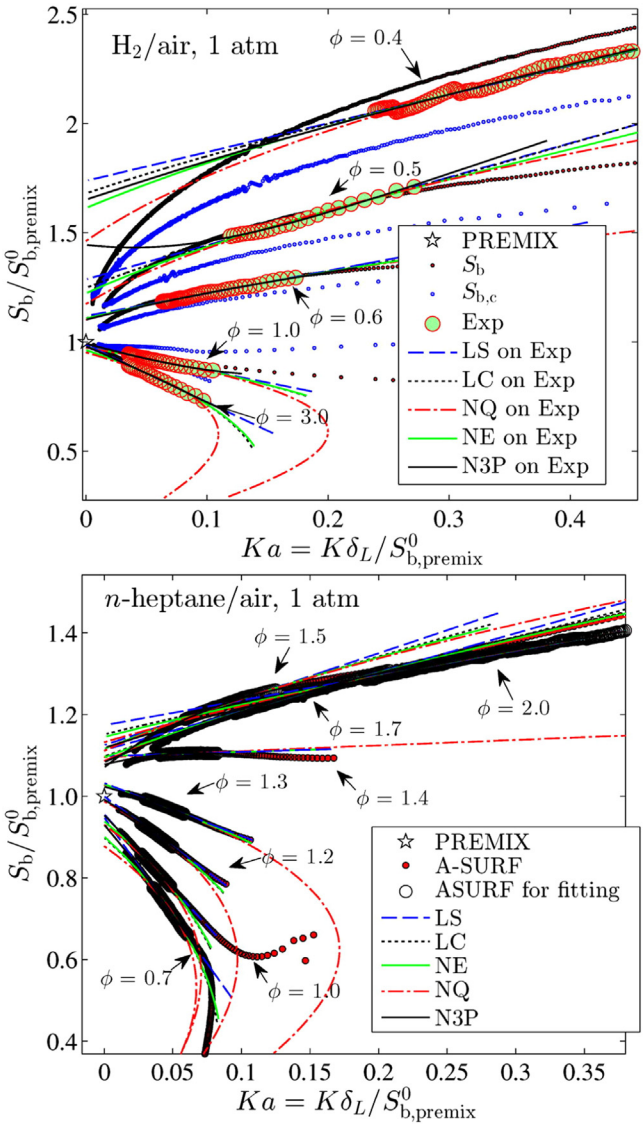

Fig. 6. Experiments, numerical simulations, linear (LX) and non-linear (NX) extrapolations of $\tilde{s}_b/\tilde{s}_b^0$ as a function of normalized stretched for SEFs of hydrogen (top) and n-heptane (bottom, for different equivalence ratios. For details on the extrapolation methods (lines), see original reference. Reprinted from [85].

small perturbations grow under the action of the prevailing flow and thermo-diffusive constraints. Under unstable conditions, a modified burning rate may result due the combined effects of stretch, curvature as well as the resulting increased area in cellular or unstable fronts. Since conditions exist in practice where flames become unstable, how should models be constructed to incorporate this phenomenon?

Early work had already identified the inherent instability of planar flames [88,89]. The analysis of Shivashinsky et al. [90] showed that CFFs should be stable for very small strains, and such is the case experimentally. Experiments in SEFs show that flames can propagate smoothly whilst the stretch due to curvature is high, then transition to an unstable surface, dominated by the presence of cells with a size of the order several times the flame thickness [33,45,91–95].

Fig. 8 illustrates how instabilities evolve from an initial perturbation to a flat flame surface. For cases where the center of curvature is in the reactants (left), (flame concave towards the reactants), heavier reactants (low diffusivity) accumulate in the

Please cite this article as: S. Hochgreb, How fast can we burn, 2.0, Proceedings of the Combustion Institute, https://doi.org/10.1016/j.proci.2022.06.029

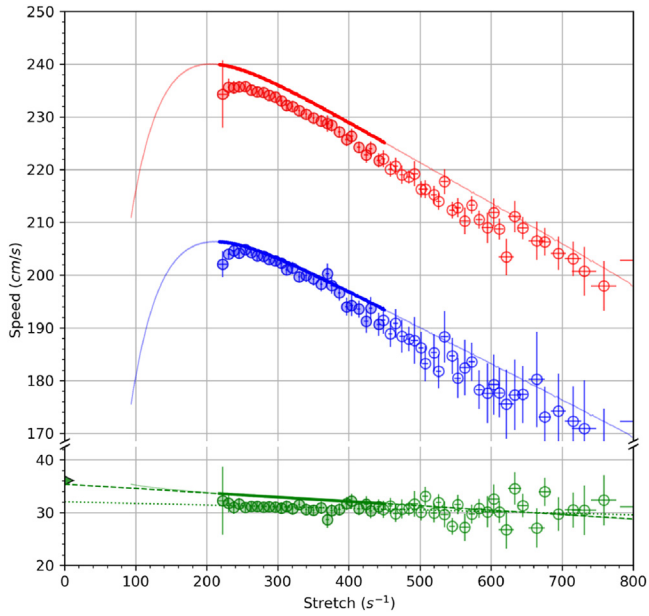

Fig. 7. Direct comparison of spatially averaged consumption speed for experimental (symbols) and DNS (lines) for methane-air flames at atmospheric conditions, $\phi = 1.0$. DNS data are represented by continuous lines. Red: $s_f = \frac{dR}{dt}$, blue: density ratio term $\frac{1}{\rho_u}\frac{d\rho_u}{dt}$ (see [14] for details), green: integrated averaged consumption speed, s_c. Linear extrapolation for consumption speed shown as dotted line and filled symbol. Reprinted from [14]. (For interpretation of the references to color in this figure legend, the reader is referred to the web version of this article.)

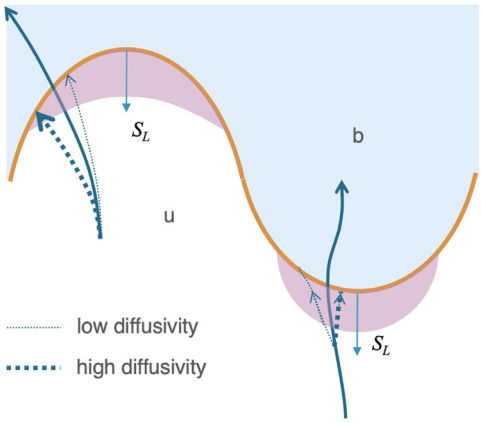

Fig. 8. Diagram illustrating the effect of differential diffusion leading to onset (or damping) of thermodiffusive instability. The flame front (orange), separates the burned (b) from unburned (u) gases. Lines show the mean streamline (solid blue), low diffusivity reactant streamline (thin dotted blue), high diffusivity reactant streamline (thick dotted line). Magenta regions show areas of limiting reactant accumulation/depletion via differential diffusion. (For interpretation of the references to color in this figure legend, the reader is referred to the web version of this article.)

high curvature region. For cases where the centre of curvature is in the burned gas (right) (flame is convex towards the reactants), lighter reactants (high diffusivity) accumulate at the cusp of the flame. If the flame is lean, additional fuel diffusion leads to higher flame speed, so that the flame advances further into the reactant, leading to a growing instability. Conversely, for low diffusivity fuels, more oxygen than fuel diffuses near the crest, leading to leaner mixtures and slower propagation speed, restoring the flame to its original position.

The conclusion is that at lean conditions, for very light fuels, such as hydrogen, the flame is very prone to instabilities, leading to fast growth of the high curvature area into the reactants. Conversely, for heavy fuels, the sensitivity to local flame instabilities is lower in the lean range. For rich conditions, a similar rationale exists, but now the limiting reactant is oxygen, so the behavior is less dependent on the particular fuel. A clear demonstration of the phenomena in flame cusps has been recently provided in [15] using DNS for lean propane flames, and in [96,97] for hydrogen flames.

A useful introduction to the topic of instabilities in general, and thermodiffusive instabilities in particular, is presented in Refs [61,98]. The recent presentation by Matalon [99] reviews the theory of the onset of flame instability clearly, as a unification of [63,100–102], based on the original work by Mark-

Please cite this article as: S. Hochgreb, How fast can we burn, 2.0, Proceedings of the Combustion Institute, https://doi.org/10.1016/j.proci.2022.06.029

stein [62,103]. The solution to the onset of instabilities for planar flames arises from the perturbation the conservation equations for flames (planar or spherical), with an assumed linear approximation for the decrease in flame speed with stretch. The solution to the perturbed equations leads to a relationship between the wavelength of the perturbation, k, and its growth rate, ω, called a dispersion relationship. The analysis for a planar flame leads to quadratic dispersion equation for $\omega(k)$, leads to the following approximation for the non-dimensional growth rate (normalized by flame convective time) as a function of wavelength (normalized by diffusive length)[99]:

$$\omega = \omega_{\mathrm{DL}} k - (B_1 + \mathrm{Ze}(\mathrm{Le}_{\mathrm{eff}} - 1)B_2 + \mathrm{Pr}B_3)k^2 \tag{22}$$

where $\omega_{\mathrm{DL}}(\sigma)$ is the positive normalized Darrieus-Landau growth rate, a weak function of the density ratio σ, k is the wavenumber non-dimensionalised by the flame thickness, the functions B_i are positive monotonic functions of σ, and Pr is the Prandtl number. Therefore, value of the second term proportional to proportional to $\mathrm{Ze}(\mathrm{Le}_{\mathrm{eff}} - 1)$ determines whether the flame propagation is stable ($\omega < 0$). In general, this means that mixtures with $\mathrm{Le}_{\mathrm{eff}}$ above a critical value are also stable for practical wavenumbers. Creta and Matalon [99,102] revised the original theory to modify the dispersion relation via a Markstein length, and found that positive strain in general has a stabilizing effect.

SEFs have been shown to be unstable over a range of specific conditions associated with the flame stretch relative to the flame time scale. Experiments in SEFs show that under certain conditions, flames can propagate smoothly whilst the strain and curvature are high. Beyond a critical radius, the strain rate is too low, and the flame transitions to an unstable surface [33,45,91–95]. Predictions of the growth rate have been made by linear perturbations to the governing equations. The predictions lead to a critical normalized radius R_c/δ_L expressed as a Péclet number, based on the rate of expansion, in [100,104,105], with the limiting condition summarized by [106] as:

$$\mathrm{Pe}_c = \frac{R_c}{\delta_L} = \mathrm{Pe}_1 + \mathrm{Ze}(\mathrm{Le}_{\mathrm{eff}} - 1)\mathrm{Pe}_2 \tag{23}$$

where the ratio $\frac{R_c}{\delta_L}$ is the smallest radius at which the instability can take place, and the functions Pe_1 and Pe_2 depend on σ and k. Beyond the critical radius, flames become unstable, and the growth rate and corresponding wavenumber control the rate of area increase. The radius at which the transition takes place depends on the multiplier of the second term $\mathrm{Ze}(\mathrm{Le}_{\mathrm{eff}} - 1)$. In general, colder, less reactive conditions at higher pressures, and small Lewis numbers lead to earlier transition, but the results are not easily generalizable, given the complex dependence on Ze and Le. Excellent agreement has been found by [106] and [107] for a range of hydrocarbon mixtures. Poorer agreement of the critical transition radius was indicated by [41] for a range of hydrogen mixtures considered (about 40–60 percent discrepancy of the radius).

The recent work of Matalon, Frouzakis, Creta and Lapenna [72,96,108–113] is starting to address the question of how one might address the interaction between the onset of instabilities and the presence of turbulence.

Most past experiments in SEFs have understandably excluded measurements when the flame transitions to instability. Nevertheless, as pointed out by Adabbo et al. [105], as well as by Bradley et al. [93] the growth rate of the flame is accelerated by the appearance of cells, and the further growth rate is proportional to $t^{1/2}$ and a factor that depends on the critical Péclet number. The details regarding flame growth rate have yet to be properly verified experimentally, although there has been at least one study on the topic [91], as well as selected DNS work [114]. This is a potential opportunity for collaboration between experimentalists and modelers, particularly if appropriate diagnostics are available to measure the spatial details of the rate of flame growth as well we heat release rate.

4. Conservation equations for progress of reaction in turbulent combustion

In the remainder of this paper, we consider how turbulent flame speeds are measured, and their relationship to the consumption and heat release rates. We start by considering the Favre-averaged conservation equations for turbulent combustion. These can for the moment be regarded as subscale averaging, so they apply equally to (uRANS) or sub-grid modelling by spatially filtering (LES) in a probabilistic framework [2–4,6,7,20,21,115]. Modeling of premixed or stratified turbulent flames involves invoking assumptions about how to average the correlations between scalars, rates and fluxes as functions of the local flow and turbulence conditions. Considering the same framework as in Section 4, the conservation equation for a Favre-average progress of reaction variable $\tilde{c}$ reads [2,4,7,115]

$$\bar{\rho}\frac{\partial \tilde{c}}{\partial t} + \bar{\rho}\tilde{\mathbf{u}} \cdot \nabla \tilde{c} = -\nabla \cdot \mathbf{T}_c^F + \nabla \cdot \mathbf{T}_c^D + \overline{\dot{\omega}}_c \tag{24}$$

where the terms for turbulent fluxes, $\mathbf{T}_c^F = \overline{\rho \mathbf{u}'' c''}$, (where $(\cdot)''$ indicates Favre fluctuations), molecular diffusion, $\mathbf{T}_c^D = \overline{\rho D_c \nabla c}$, and reaction $\overline{\dot{\omega}}_c$ require modelling. The averaged or filtered terms indicated by $(\tilde{\cdot})$ do not in general correspond to the values of the operators evaluated at averaged or filtered variables. Departures from the averaged temperature create significant deviations in the reaction rates of most scalars, which depend exponentially

Please cite this article as: S. Hochgreb, How fast can we burn, 2.0, Proceedings of the Combustion Institute, https://doi.org/10.1016/j.proci.2022.06.029

on the local temperature. The modeling of fluctuating and reaction terms requires an understanding of the fluctuation of the progress of reaction variable, typically via a probability density function (pdf) and closure equations for the higher moments of the distribution.

Alternative formulations can be based on the flame surface density and its propagation, equivalent to those of progress of reaction for premixed flames. In these formulations, the flame surface density Σ is defined as an isosurface at $c = c^*$. The mean flame surface density is estimated from a conditional gradient of progress variable [7,26] as $\Sigma = \overline{|\nabla c|\delta(c - c^*)} = \overline{|\nabla c|}_{c=c^*} P(c^*)$, where $\overline{|\nabla c|}_{c=c^*}$ is the conditional average of $|\nabla c|$ at $c = c^*$, and $P(c^*)$ is the probability to find $c = c^*$ at a given location. The mean reaction rate is often modelled as the conditioned mean burning rate $\overline{\dot{\omega}}_c = \overline{\rho s_c \Sigma}$, where s_c is usually assumed to be s_L^0.

The concepts of isoprogress of reaction variable c and flame surface density Σ are reasonably accessible to the experimentalist. Additional terms in the balance of progress of reaction such as 3D diffusive fluxes, reaction rates or scalar dissipation rate are significantly harder to measure quantitatively.

Given the ubiquitous idea of the laminar flame speed, it is often useful to work with the measurement of turbulent speeds when discussing turbulent premixed flames. One can divide Eq. (24) by $\bar{\rho}|\nabla \tilde{c}|$ to obtain a balance of speeds:

$$s_T = \frac{1}{|\nabla \tilde{c}|} \frac{\mathrm{D}\tilde{c}}{\mathrm{D}t} = s_D + s_F + s_R \tag{25}$$

where the left hand term s_T is a mean convective displacement speed, and the three terms on the right can be once again identified with molecular diffusion, turbulent flux and reaction rate. This formulation is useful to understand the balance of terms in the conservation equation for $\tilde{c}$, yet one needs to be very clear in defining how to compare simulated turbulent flame speeds with values of quantities obtained from experiments. In particular, many turbulent flame propagation models rely on the ability to express the unclosed reaction term as a function of the local turbulence parameters, in a manner that ideally is independent of flame flow geometry. However, whereas reaction terms may be geometry independent, diffusive flux terms depend strongly on geometry via the resulting velocity fields.

Extensions and variations of models are required for systems involving stratification or differential diffusion. Many models exist for the closure of the various unclosed source terms that arise from the separation of mean and fluctuation (as in RANS) or by filtering (in LES). A clear description of the connection between turbulent combustion models and how they relate to each other is available in the still excellent review by Veynante and Vervisch [7]. Many extensions have been added through the years for the role of stratification [21], the role of differential molecular diffusion [116], and the effect of heat release [4,5,117,118]. Many or most of the models for the unclosed terms in RANS or LES equations over the past 20 years have been provided by extracting results from DNS. These closures usually take the form of algebraic or dynamically calculated expressions for the unclosed reaction and diffusion terms in both the mean or higher moment conservation equations. The final validation for proposed models must be done against existing experiments in turbulent flames.

Previous reviews have surveyed the wealth of experiments used for validation of increasingly complex situations for turbulent flames [9,22,119]. In this paper, we focus on experiments designed to extract the turbulent flame speed in premixed flames. In Section 5, we survey the current understanding of experimental measurements of turbulent flame speeds. For the experimentalist, we try to clarify the importance of understanding the precise definitions of what must be measured in order to provide suitable validation datasets. For the modeler, we try to explain what actually has been measured and some of the difficulties arising in the interpretation of results.

5. Measuring premixed turbulent flame speeds

Measurements in turbulent premixed flames have been performed for countless cases under a variety of geometric conditions, with the objective of comparing LES or RANS-based models. Comparisons of simulation results with experimental values of scalars and velocities are useful indicators of whether models can correctly capture flame location and structure in both industrial and laboratory flames, particularly under unsteady conditions, as reviewed in [7,22,120,121]. In general, most detailed measurements of scalars and velocities have been extracted from statistically stationary flames, as flames in unsteady engines or expanding flames cannot be easily targeted by optical diagnostic techniques.

However, decomposing the influence of small scale turbulence from mean flow fields is made harder in the case of practical flames with large scale vortices designed for stability, as in swirling or dump-cavity stabilized flames. Instead, a number of experiments have been performed under conditions that more closely approximate flame propagation for ideal isotropic turbulence conditions, where in theory the geometry does not significantly affect the imposed small scale turbulence.

In these experiments, one hopes to recover a relationship (ideally universal) between effect of small scale turbulence and the burning rate, which can be incorporated into models, or used for model validation. For an ideal flame brush propagating in one-dimension (see Fig. 9), this is possible, as integration of Eq. (24) across a statistically stationary

Please cite this article as: S. Hochgreb, How fast can we burn, 2.0, Proceedings of the Combustion Institute, https://doi.org/10.1016/j.proci.2022.06.029

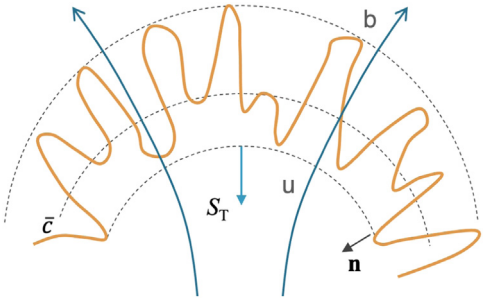

Fig. 9. Schematic diagram for propagation of a flame brush into the unburned (u) gases, showing streamlines (blue), instantaneous flame (yellow) and isocurves for mean progress of reaction. Note that in general, isocurves are not parallel. (For interpretation of the references to color in this figure legend, the reader is referred to the web version of this article.)

flat flame brush yields:

$$\tilde{u} = s_{T,0} = s_R = \frac{1}{\rho_u} \int_0^1 \frac{\overline{\dot{\omega}}_c}{|\nabla \tilde{c}|} d\tilde{c} \tag{26}$$

where ρ_u the density of reactants and $s_{T,0}$ is the measured displacement velocity at the leading edge, and where the terms associated with divergence of turbulent and laminar diffusion fluxes disappear. This happens because diffusive fluxes of c become zero at both leading and trailing edges, by definition, and the symmetry of the flat flames means that the net cross-streamtube flux is also zero. In this case, the consumption speed becomes identical to that of the leading edge speed, as expected from conservation equations. However, it has not proved possible to produce such a stable, one-dimensional flat turbulent flame in practice. As reviewed in [122], past geometries considered for measuring flame speeds are: (a) stabilized flames in incoming flows with controlled turbulence such as Bunsen, impinging or opposed, V-, and diverging low-swirl flames; and (b) unsteady spherically propagating flames in vessels with turbulence generated by fans prior to ignition. Instantaneous and mean flame areas have usually been determined by 2D isoscalar imaging, such as Mie scattering [123,124], Rayleigh scattering [125], OH PLIF [126], and in some cases, flame natural luminosity [12,127,128].

5.1. Stabilized Bunsen flame (SBF) measurements

Bunsen flames have been most popular for such measurements, starting with Damköhler's experiments [12]. Consider a control volume $\mathcal{V}_\delta$ which envelopes the entire flame brush, while anchored at the base of the jet. The overall mass flow rate of reactants $\dot{m}$ must equal the total rate of reactant consumption when the whole flame brush is enclosed by a control volume.

$$\dot{m} = \rho_u \check{s}_{T,0} A_0 = \check{\rho}_{\tilde{c}} \check{s}_{T,\tilde{c}} A_{\tilde{c}} = \dot{\Omega} \tag{27}$$

where the mass flow rate is of course conserved across the envelope of the flame. The check ($\check{\cdot}$) symbol notation here indicates that the corresponding speed is implicitly averaged along the flame brush contour at an iso-$\tilde{c}$. The corresponding velocity, $\check{s}_{T,0}$, is often called a global rate of burning, $s_{T,G}$. Notice that each iso-$\tilde{c}$ surface is connected by mass conservation to a corresponding density and area.

In the literature, there are large discrepancies among measurements of the global quantity $s_{T,G}$ in typical Bunsen flames. Significantly, the choice of iso-$\bar{c}$ curves tends to vary between investigators, from one near the leading edge ($\bar{c} = 0.01 - 0.1$) [123,124] to near the peak luminosity around $\bar{c} = 0.5$ [12,127,128]. Oddly, there is typically no attempt to correct for the correspondingly changed mean density at different $\bar{c}$ values. Further, both the angle between the fresh gas velocity and flame brush and the thickness change significantly around the surface of the flame, which means that the mass flow rate per unit area (and thus the local turbulent flame speed and consumption rate) is far from uniform around the flame brush.

These considerations have in the past inspired a number of studies by Shepherd, Bray, Kostiuk, Cant and coworkers [129–133], who measured the separate diffusive flux terms in the balance equation Eq. (25) using local laser-Doppler anemometry (LDA) in order to close the balance of the conditional terms in the thin flame regime for various geometries, including Bunsen, impinging flames and diverging low-swirl flow flames. At least one study [132], succeeded in balancing the terms for turbulent flames to obtain the consumption speed using measurements of velocity and confirmed them by independent measurements of flame surface density, with the assumption of thin laminar flames with constant flame speed. At the time, these painstaking studies were particularly difficult, as LDA measurements are point-wise. We suggest that there is an opportunity to revisit these experiments using modern high speed stereo PIV to extract similar information for a wider range of conditions.

Driscoll [122] reviewed the ability of simulations to capture the behaviour of turbulent flames stabilized as Bunsen, V-flames, low-swirl, counterflow flames, and spherical flames, showing significant disagreement in the measurements regarding which reference areas to use and how to estimate velocities. Further, he observed that different authors used different definitions of turbulent flame speed and turbulent burning rate, which are sometimes incorrectly conflated. In an attempt at quantifying the differences between measurements, we have in this paper selected datasets filtered by type of fuel (methane only), device (Bunsen only), and operating conditions (atmospheric), and cases in which it was possible to reconstruct the original $s_{T,\tilde{c}}$ and l_0 chosen, so that the normalised values are consistently comparable. Even if the reference areas selected are typically uncorrected for mean density at

Please cite this article as: S. Hochgreb, How fast can we burn, 2.0, Proceedings of the Combustion Institute, https://doi.org/10.1016/j.proci.2022.06.029

Table 1
Selected measurements of premixed turbulent flame speeds of methane-air mixtures in steady Bunsen burners (SBFs) at atmospheric pressure and temperature.

Label	Ref.	ϕ	$\hat{u} = u'/s_L$	$\hat{\Lambda} = l_0/\delta_L$	$\bar{c}$	Measurement
Cheng88	[134]	0.7∼1.0	0.8∼1.8	24.5∼45.9	0.5	Mie
Cheng91	[133]	0.7∼1	0.8∼1.9	51.4∼85.7	0.5	Mie
Kobayashi96	[95,123,124]	0.9	0.3∼11.3	18∼212	0.5	Schlieren
Shepherd98	[135]	0.75∼0.95	0.68∼1.32	24∼75.2	0.5	Mie
Kobayashi05	[136]	0.9	0.4∼9.5	34∼132	0.1	OH-PLIF
Filatyev05	[137]	1	0.28∼8.5	8.9∼36.6	0.05,0.5	OH-PLIF
Yuen09	[138–140]	0.6∼1	2.7∼24.1	8.9∼30.2	0.05, 0.2, 0.5	Rayleigh
Troiani13	[141]	0.8∼1	2.2∼6.4	34.9∼96.3	0.05,0.5	OH-PLIF
Tamadonfar14	[142,143]	0.7∼1	1.8∼12.3	12.8∼40.2	0.05, 0.5	Rayleigh
Tamadonfar15	[125]	0.7∼1.35	2.4∼10.4	19.9∼47.1	0.05, 0.5	Rayleigh

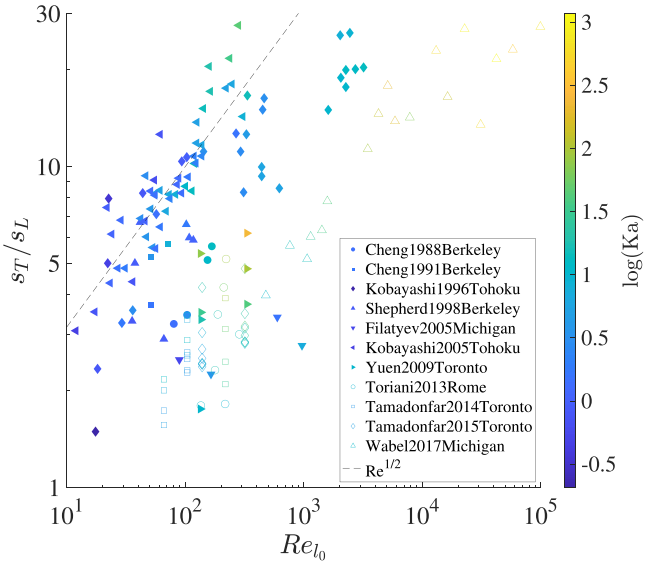

Fig. 10. Measurements of normalized global premixed turbulent flame speeds of methane-air mixtures in Bunsen burners $s_{T,\bar{c}=0.5}/s_L$ at atmospheric pressure and temperature as a function of $\mathrm{Re}_{T,l_0} = u' l_0/\nu$, and $\mathrm{Ka} = (u'/s_L)^{3/2}(l_0/\delta_L)^{-1/2}$. All points selected for values measured at $\bar{c} = 0.5$, to allow full comparison.

$\bar{c} = 0.5$ (see Eq. (27), at least those are consistent with each other.

Table 1 shows that the data spans ranges of $\hat{u} = u'/s_L$ from below one to 24 and $\hat{\Lambda} = l_0/\delta_L$ from 10 to 200 (in this section, the values of s_L and δ_L refer to unstretched values), spanning from the thin flame through the disrupted flame regime. Calculated values of global turbulent flame speeds, $s_{T,\bar{c}=0.5}/s_L$, from this combined dataset are shown in Fig. 10. The primary purpose of the comparisons is to show that there are significant differences between measurements that in principle should be very similar. The scaling based on $\mathrm{Re}_{T,l_0} = u' l_0/\nu \approx \hat{u}\hat{\Lambda}$ is inspired by the various available correlations in which a power of u' often non-dimensionalized as Re_T. At zero turbulence, measurements should converge to the laminar flame speed. At high turbulence, [122,150], simple transport theory based on a dominant eddy diffusivity suggests a dependence on $Re_{T,l_0}^{1/2}$ [12,115]. Alternative analyses [151,152] suggest a dependence on a negative power of a Karlovitz number, often defined as $\mathrm{Ka} = \hat{u}^{3/2}\hat{\Lambda}^{-1/2}$. The choice is not unique, and sometimes a Damköhler number is used instead, where $\mathrm{DaKa} = \mathrm{Re}_T^{1/2}$. The correlations in Fig. 10 are apparent for the data extracted from each single investigation. However, there are significant deviations between measurements from different investigators. The values of normalized $s_{T,G}$ can also be plotted against $\hat{u}$ and $\hat{\Lambda}$ with equally good (or poor) agreement. The differences arising from different choices in iso-$\bar{c}$, have been eliminated by filtering the data to only those obtained at $\bar{c} = 0.5$ in the figure, and the same base properties were used for the calculation of s_L and Re_{T,l_0}. It is possible that different burner flow configurations can lead to different mean flow di-

Please cite this article as: S. Hochgreb, How fast can we burn, 2.0, Proceedings of the Combustion Institute, https://doi.org/10.1016/j.proci.2022.06.029

vergence, thus different distributions of velocities around the flame brush and different mean global flame speed values. Further detailed measurements or data analysis revealing detailed fluxes would be welcome to resolve the discrepancies.

There is a smaller data set of measurements for different fuels in turbulent Bunsen flames, including those with different diffusivity on syngas [153] and hydrogen [154], for example. However, it was not possible to directly compare the various operating conditions directly given the sparsity of the measurements in this exercise.

These comparisons show that that not only are there significant discrepancies in the measurements from Bunsen flames, even after filtering for comparable experiments, but also that there is a need for further detail in reporting these types of data, including compiling detailed mean velocities and their moments in space, as well as mean progress of reaction and related turbulent fluxes for proper comparisons with model predictions. Datasets from previous experiments developed have in some cases been used for comparison with LES models [155,156], and subsets of data have been used to determine the alignment of strain and flame surface [157], as well as mean normalised strain functions at the flame surface [137]. Yet the lack of systematic fine grained simultaneous measurements of velocity moments and progress of reaction makes it difficult to directly assess the fidelity of different subgrid models, except by relatively global comparisons. There appears to be a case for revisiting turbulent flame speed measurements in different geometries using stereo velocity and progress of reaction measurements to quantify the different terms (reaction, diffusion) as in past experiments [129–133], but using modern techniques that might allow inspection of a large domain in the flame, and comparison of individual terms in the $\tilde{c}$-balance. Such measurements and comparison with simulations would allow a coherent representation of the mean consumption and displacement speed as a function of local and mean turbulent conditions, which could also be extended to less well studied mixtures at non-unity Lewis numbers.

5.2. Spherically expanding turbulent flames (SEF)

As in the case of laminar flames, a second source of measurements of the effect of turbulence are spherically expanding flames. In this configuration, there is no mean flow, and the flame propagates through a uniform premixed mixture. The burning rate can be extracted from the rate of pressure rise in the vessel or from visual observations of the rate of growth of the leading edge, when the pressure rise is low. Subtraction of the mass conservation equation from the balance of $\tilde{c}$ for the expanding flame using a control volume across the flame brush volume, V_δ, leads to:

$$\dot{\Omega} = \rho_u \tilde{s}_{T,0} A_0 - \frac{\partial}{\partial t} \int_{V_\delta} \bar{\rho}(1-\tilde{c})\, dV \tag{28}$$

where $\tilde{s}_{T,0}$ is the mean displacement velocity relative to the velocity of the leading edge of the flame front $\tilde{s}_{F,0}$, and $\dot{\Omega}$ is the total reaction rate. The diffusive terms disappear at the leading and trailing edges, and the convective flux term associated with (1- $\tilde{c}$) term disappears at the burned gas boundary. The last integral in the RHS is negligible if the rate of change of the mean unburned (and thus burned) mass in the flame brush is small during flame propagation. Finally, an approximation is often made between the rate of mass burned and the volumetric expansion of the burned gases, so that under these conditions,

$$\frac{dm_b}{dt} = \rho_b \frac{dV_b}{dt} = \rho_b A_b \frac{dR_b}{dt} = \dot{\Omega} \tag{29}$$

$$\tilde{s}_{T,0} \approx \frac{\rho_b}{\rho_u} \frac{dR_b}{dt} = \frac{\dot{\Omega}}{\rho_u A_0} \tag{30}$$

Differences between A_0 and A_b are either corrected for or neglected in schlieren measurements, and the radius equivalent volume of burned gases, is sometimes adjusted to accommodate the turbulent flame thickness at a particular instant.

The first approximation in Eq. (28) shows that the turbulent flame speed as determined by Eq. (30) should equal that of the consumption rate, so long as that the total mass of unburned gases remains constant in the flame brush. The turbulent flame brush thickness has often been measured to grow either linearly or with the square root of time [150,158], so the term in general should not be zero, but there have been few estimates of its magnitude. The studies in [159] sought a solution to the issue by selecting a mean radius of the flame as a value where the term is intentionally zero, so that the mass of burned and unburned gases are balanced as observed from Mie scatter images. This radius is in general different than the leading edge or schlieren radius. However, a correlation between the rate of change of the Mie-mean and schlieren radius was established to be within 10% of each other for experiments with propane [159]. Most other studies have used the mid-point of flame location based on schlieren measurements without accounting for the mean density change or accumulation terms described above. This is clearly area requiring further confirmation and analysis for more general situations.

The studies shown in Table 2 were selected from those at atmospheric conditions for methane-air mixtures, and which offered sufficient information to be directly comparable. The ranges of normalised turbulent velocity, $\hat{u} = u'/s_L$ are somewhat larger than those in Bunsen flames, and the normalized length scales $\hat{\Lambda}$ are significantly larger

Please cite this article as: S. Hochgreb, How fast can we burn, 2.0, Proceedings of the Combustion Institute, https://doi.org/10.1016/j.proci.2022.06.029

Table 2
Selected measurements of premixed turbulent flame speeds of methane-air mixtures for spherically expanding flames (SEFs) at atmospheric pressure and temperature.

Label	Reference	ϕ	$\hat{u} = u'/s_L$	$\hat{\Lambda} = l_0/\delta_L$	Measurement	R (mm)
Abdel-Gayed84	[144]	0.72∼1	10∼40.5	741∼1232	Schlieren	/
Liu11	[145]	0.8	4.4∼15.4	680∼1900	Luminosity	>20
Chaudhuri12	[146,147]	0.9	4.4∼16.8	80∼210	Schlieren	12∼22
Chaudhuri15	[148]	0.9	4∼10.3	80∼210	Mie	3∼13
Jiang16	[149]	0.9	2.4∼31.1	680∼2800	Schlieren	25∼45

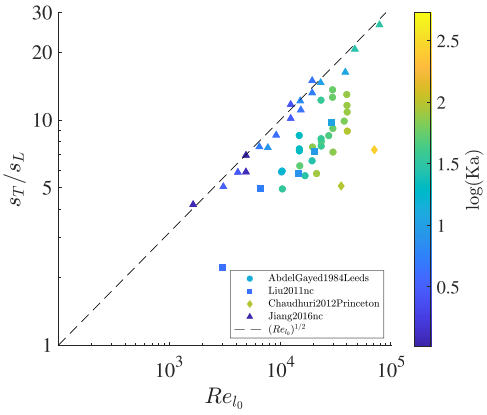

Fig. 11. Measurements of premixed methane turbulent flame speeds in spherically expanding flames at atmospheric pressure and temperature as a function of function of $\mathrm{Re}_T = u'l_0/\nu$, and $\mathrm{Ka} = (u'/s_L)^{3/2}(l_0/\delta_L)^{-1/2}$.

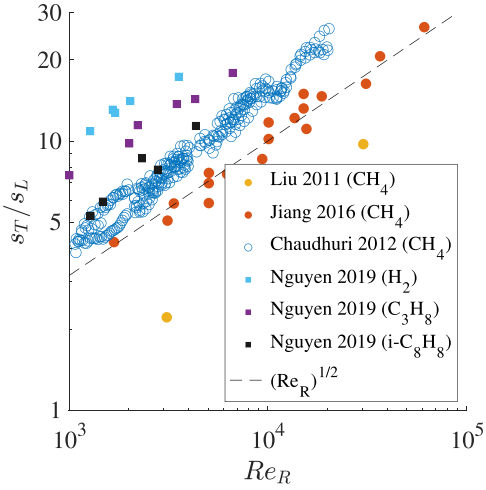

Fig. 12. Measurements of premixed turbulent flame speeds in spherically propagating flames at atmospheric pressure and temperature as a function of Reynolds number based on mean line-of-sight schlieren flame radius (circles), R: $\mathrm{Re}_T = u'R/\nu$. Data for Liu_2011 [145] and Jiang_2016 [149] are for a fixed R and different u' values. The data in squares is by [165] for different fuels at different conditions.

than those in Bunsen burners. The results for the normalized flame speed $\hat{s}_T = s_T/s_L$ are shown in Figs. 11 and 12 as a function of the integral length and radius-based Reynolds numbers. The main point of the comparison is to show that there are still significant disparities between measurements, even for very similar nominal operating conditions. Clearly, the results for methane mixtures show that there is a general correlation with $\mathrm{Re}_T^{1/2}$ as discussed for Bunsen flames. However, a whole range of correlations have been proposed for SEF flames based on Re_T, Ka, $\hat{u}$ and Markstein or Lewis numbers, with comparable success given the large scatter [30,116,160].

A robust correlation has been found by several authors with the square root of the radius-based Reynolds number, $\mathrm{Re}_R^{1/2}$. The assumption is indeed supported the scatter plot in Fig. 12, which includes the data in Table 2. The suggested scaling was recently attributed to the role of instabilities [147,161]. However, other theories that do not directly invoke instabilities have successfully captured the growth of the radius as a function of time in turbulent flames, for example using a flame speed closure assumption [150,162,163] or scalar dissipation rate modeling based on DNS closures [164]. Additional data by [165] for hydrogen, propane and isooctane, are discussed further in Section 5.3.

We conclude from this short section on the measurement of turbulent flame speeds of methane at ambient conditions that:

(a) For conditions where there is steady state in the mass contained in an enclosed flame brush, it follows that the mean displacement turbulent speed equals consumption speed. However, there are experimental difficulties in verifying the conditions needed for the balance, for example the mean density at the relevant isosurface needs to be properly corrected;
(b) There is a wealth of data from turbulent SEFs that indicate various correlations between s_T/s_L and turbulent quantities. In particular, there is good agreement for measure-

Please cite this article as: S. Hochgreb, How fast can we burn, 2.0, Proceedings of the Combustion Institute, https://doi.org/10.1016/j.proci.2022.06.029

ments of flame speeds, with scaling based on the radius Reynolds number $s_T/s_L \sim \mathrm{Re_R}^{1/2}$ within the ranges measured. However, these relationships are not universal for all mixtures and conditions, which indicates different regimes which need to be captured;

(c) For SBFs, there is poor agreement between experiments that are nominally similar. The latter may be because of spatial non-uniformities, differences in choice of reference area, and dependence of the local values of s_T on the mean flow and strain rate;

(d) The role of the integral turbulent scale in either SEFs or SBFs remains unclear, as the ranges considered for variation in SBFs has been small [137], and those for SEFs are typically fixed by fan arrangements. Yet from the considerations above, scale effects appear to be dominated by the radius growth, at least in some regimes.

Measurements of s_T between SEF and SBF appear to not be directly comparable, as neither method directly measures the consumption speed for a given set of similar mixtures and turbulent conditions. Whilst often SEF measurements are extracted at a particular radius for different values of u', s_T is shown to *vary* with radius, so it cannot be generally associated with a value of $(\hat{u}, \hat{\Lambda})$. The measurement of two dimensional flame position and 3D velocity is possible, and recently attempted [32,166], to help better understand how flame surface density and flame brush thickness evolve. Sensible comparisons might be drawn using more fundamental models or turbulent simulations, which could target the time history of flame radius, flame brush evolution and velocity fields. That sort of comparison has been occasionally done using both LES and DNS for SBFs and SEFs [155,167,168], but there is an important message for experimenters to create and maintain shared databases that could further help model comparison and analysis. Data acquired from previous experiments would be very valuable if the original detailed measurements of radius, flame brush thickness and velocities had been measured and made available in the form of archival databases.

5.3. The role of Lewis number on flame propagation in turbulent SEFs

So far we have only examined the behavior of methane mixtures, in order to allow fair comparisons between datasets. Can we compare datasets for other fuel mixtures? Surely there should be large databases of measurements for the engine reference fuels isooctane and n-heptane? And what might be the role of Lewis number?

Early work on the effect of Lewis number on the propagation of spherical turbulent flames came from Karpov and Severin [169], Kido [170–172], and extensive work by Bradley et al. [30,151,173], and more recent work has been added by Law and coworkers [147,166] and Shyy et al. [149,174]. Here we include samples of the later work, as we were able to verify that the range of conditions (pressure, temperature and local flame radius) were comparable to other cases. Ideal comparisons would involve the full history of radius as a function of time for fair comparisons.

There are countless correlations for turbulent flame speeds, either as a function of the non-dimensional turbulent flame speed and length scale, or as a function of the relevant non-dimensional numbers. In general normalized flame speeds increase as a positive power of the turbulent velocity, typically expressed as Re_{T,l_0}, but sometimes as a negative power of a suitable Ka, and less frequently, including a negative power of Le, or as best fit functions of a suitable Markstein number [150–152]. A few of them have concerned themselves specifically with the role of Lewis numbers. For example, Bradley et al. [30,151] proposed correlations for the normalized turbulent burning velocity as $\hat{s}_T = a\hat{u}(\mathrm{K_m Le})^b$, where $\mathrm{K_m} \propto \hat{u}^2 Re_{T,l_0}^{-1/2}$, and a and b are both functions of Le for the particular mixture.

A study by Nguyen et al. [174] on the NCU-Taiwan data connected data from propane and hydrogen from SEFs. to those of Jiang et al. [149] suggested correlation $\hat{s}_T = C(\frac{\mathrm{Re}_R}{\mathrm{Le}})^{1/2}$, In their data analysis, this appears to collapse the data for different fuels onto a single curve. The data in [174] are shown as squares in Fig. 12 for the different fuels, showing their different sensitivities to Le [1]. A few studies [116,175] successfully used the leading points theory of Zel'dovich et al. and Kuznetsov et al. [61,176] to make suitable predictions of the propagation in turbulent SEFs for a variety of mixtures with different Lewis numbers, based on the data of Karpov and Severin [169]. The theory considers how differential diffusion changes the temperature and thus the burning rate of a spherical flame unit associated with the leading edge of the flame. Studies by Muppala et al. [177] used the asymptotic version of the leading points methods in predictions of hydrogen mixture flame measurements, but the predictions did not entirely succeed in capturing the behavior of flame speeds. The subject is ripe for an in-depth reexamination of the original experimental data, in the light of the interest in the subject of light fuels.

[1] The data plotted in Fig. 12 were extracted from the original studies in [149] and [174], but show slight differences in the calculated Re_R, which may be due to different choices for mixture properties. In general one would expect the $\hat{s}_T$ for i-octane and propane to fall below those of methane, which is not the case here.

Please cite this article as: S. Hochgreb, How fast can we burn, 2.0, Proceedings of the Combustion Institute, https://doi.org/10.1016/j.proci.2022.06.029

5.4. The mystery of the missing flame area

One of the enduring assumptions in turbulent premixed combustion has been Damköhler's first hypothesis, that at moderate levels of turbulence (Ka≤100), the rate of reaction increase is a result of the increase in the area of a relevant progress iso-scalar, so that a factor I_0 can be defined,

$$I_0 = \frac{s_T/A_T}{s_L/A_L} = \frac{\dot{\Omega}}{\rho_u s_L A_T} \tag{31}$$

where the area A_T is the corresponding mean area of a suitable isosurface marking the flame, A_L.

Measurements of isosurfaces in SBFs are typically done using 2D imaging of Mie scatter particles, OH or Rayleigh scattering. These have been shown to be suitable markers except in the highest turbulence cases, in which the inner flame zone may be smeared. In selected experiments in Bunsen flames, the global measured mass flow rate going through the flame $\dot{m}$ was found to be larger than the theoretically possible burning rate $\rho_u s_L A_T$ based on the unstretched laminar flame speed and estimated 2D flame surface density extrapolated to 3D, implying that the value of I_0 is a factor of 2–5 [126,140]. Expected uncertainties in 2D measurements are of the order of 20–30%, and differences between 2D and 3D area estimations could be responsible for another 30% [179,180]. The role of experimental uncertainties is further discussed in [9], but the estimated corrections do not quite reach the larger factors experimentally observed. DNS simulations which report flame isosurface areas suggest that 3D turbulent area track the increase in reaction rate [181,182] within 10 percent even at relatively high levels of turbulent Karlovitz numbers, but it is still unclear whether the small scales in DNS are entirely representative of larger flames.

Recent measurements of 3D surfaces in turbulent SEF [178] have shown that there are large differences in the I_0 values determined from 2D and 3D surfaces. Fig. 13 shows the factor I_0, measured as the ratio of the normalised turbulent velocity, s_T/s_L, as determined from the heat release via pressure records, to the normalized area of the 3D isosurface, A_T/A, where A_T was measured using scanning Mie scatter, and A is the mean burned gas area. The values in the figure show that the factor I_0 hovers around unity for methane, but reaches much larger values for hydrogen. The conjectured reason is the large difference in instability behaviour between in the cases for methane mixtures ($Le \approx 0.7$), and for the lean cases with hydrogen (Le ≈ 0.3). The discussion in Section 3.5 suggests that lean hydrogen mixtures are extremely thermodiffusively unstable, as the regions of high convex curvature towards the reactants accelerate further, propelled by the higher fuel mass fractions transported to those regions via differential diffusion, leading to growing instabilities. Section 6 further examines the recent findings from DNS regarding the role of Lewis numbers.

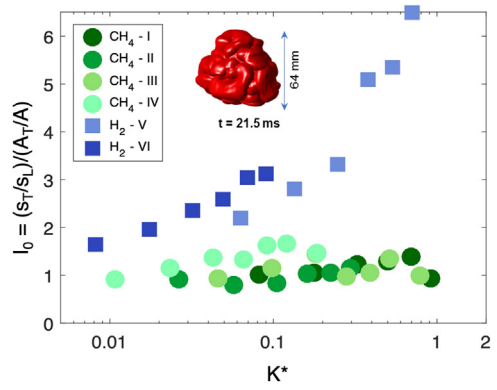

Fig. 13. Ratio of normalized measured turbulent velocity using pressure data ($s_{T,m}/s_L$) to the 3D measured area ratio (A_T/A) based on 3D scanning measurements, as a function of the modified Karlovitz stretch factor, $K^* = \frac{1}{4}\left(\frac{u'}{s_L}\right)^2 Re_{l_0}^{1/2}$. Data from [178]. Inset shows rendering of a 3D flame at a particular instant. Cases I-IV for methane go from lean to rich at pressures of 1 to 5 bar; Cases V and VI for hydrogen are for equivalence ratios of 0.3 and 0.4, respectively, at 5 bar.

6. DNS of turbulent flames: Lewis number

DNS for both laminar and turbulent flames currently provide the backbone for the understanding of diffusive-reactive phenomena in combustion, including the role of stretch, curvature instabilities, as well as by providing quantitative input for a range of parameterized closures and subgrid models for premixed and partially premixed combustion [55,183–187].

These cannot yet capture all the necessary length scales or boundary conditions of most experiments at realistic scales, with a few exceptions for small-scale burners (e.g. [188,189]). A large number of DNS simulations have formed the basis for sub-grid models for a large number of situations using LES and RANS modeling [55,183–187,190]. These models are currently evolving to include improvements to incorporate the unusual properties of hydrogen mixtures and instabilities [109,191].

There are hundreds of papers covering many different aspects of DNS of laminar and turbulent flames, and there is not enough space in this review to discuss the vast literature on the subject. From the early simulations of Haworth and Poinsot [192], Rutland and colleagues [193], through the work of Cant, Chakraborty, Swaminathan, and Klein [190,194–197], and the more recent work of Savard and Blanquart [198], Aspden et al. [199,200], and Lipatnikov and colleagues [201,202], it has been

Please cite this article as: S. Hochgreb, How fast can we burn, 2.0, Proceedings of the Combustion Institute, https://doi.org/10.1016/j.proci.2022.06.029

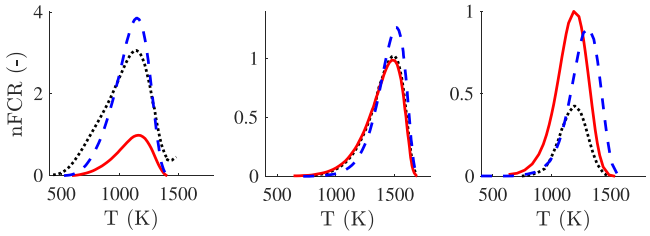

Fig. 14. Conditional means of fuel consumption rate for DNS flames of H_2 ($\phi = 0.4$, Le ≈ 0.37) (left), CH_4 ($\phi = 0.7$, Le ≈ 1.0)(center) and dodecane (right) ($\phi = 0.7$, Le ≈ 4.4), normalised by the peak consumption rate for the laminar case, for simulations at the same Ka = 36. Black dotted lines are the conditional means from the simulations, red solid lines are the one-dimensional laminar flame profile, blue dashed lines are the one-dimensional unity Lewis number results. See original studies for further details [181,199,200]. (For interpretation of the references to color in this figure legend, the reader is referred to the web version of this article.)

well known that the Lewis number plays a key role in the propagation of turbulent flames.

In this final section, we review the role of stretch via curvature and differential diffusion on the DNS-resolved burning of three different representative fuel mixtures: hydrogen, methane and a dodecane, which cover very low, unity and very large Lewis numbers, respectively. The behavior of the reaction rate is compared under similar turbulence conditions, to understand the roles of differential diffusion and chemistry.

Aspden and coworkers [199,200] have produced full chemistry simulations for lean fuel mixtures fuels with very different Lewis numbers, at moderate and high Karlovitz numbers, defined as $\mathrm{Ka} = \hat{u}^{3/2}/\hat{\Lambda}^{1/2}$, for domains $(10 \times 10 \times 80)\delta_L$. Fig. 14 shows normalized fuel consumption rates for hydrogen (left), methane (center) and dodecane (right) mixtures at Ka = 36 (black) as a function of temperature, normalized by the values of the laminar case (red). Also plotted are the results for reference mixtures calculated with equal diffusivity (blue). Starting with the results for methane mixtures with unity Le, it is clear that the inner structure of the flame does not change with turbulence. In contrast, the reaction and heat release rate for hydrogen are significantly affected by turbulence: the conditioned fuel reaction rate increases about 4 times relatively to the laminar value for moderate Ka. Finally in the case of dodecane, the reaction rate decreases relatively to the laminar case for increasing turbulence. The heat release rates (not shown) generally mirror the behavior of the fuel consumption rate. A number of other DNS studies paint a similar picture for the dependence of the conditional rate of reaction on Le and Ka [198,203–205]: for lean mixtures with low Lewis number fuels, the rate of reaction increases markedly with turbulence, owing to thermodiffusive instabilities that change the local stoichiometry and increase the reaction rate. In the case of high Lewis number fuels, the opposite effect is true, but the effect tends to be milder, as it is weighted by the more moderate reaction rate change with

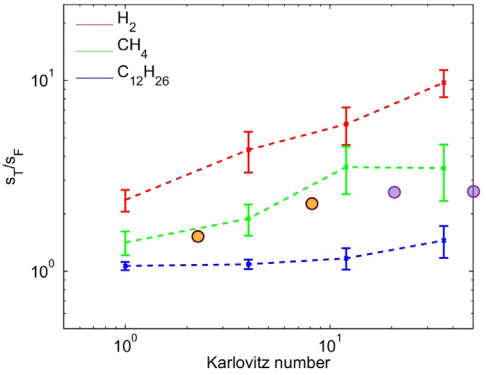

Fig. 15. Consumption-based global turbulent flame speeds as a function of Karlovitz number, normalised by the steady unstrained flame speed for lean flames of H_2, CH_4 and large hydrocarbons. Crosses denote nominal averages, and the vertical lines indicate one standard deviation of the fluctuations observed once the flame has become established. Lines: [200], detailed chemistry, orange circles: iso-octane detailed chemistry [204], magenta circles: n-heptane two-step mechanism [205]. The different studies use slightly different domains, which affects the absolute value of s_T.

stoichiometry compared to hydrogen. The effect of turbulence on the burning rate is shown in Fig. 15 for hydrogen, methane and large hydrocarbon fuels, according to three different DNS realisations [200,204,205]. Once again, the strong dependence on Lewis number is apparent from the simulations, with the largest sensitivities associated with low Lewis number lean H_2 mixtures. The very strong dependence of turbulence reaction rate on Le number is of course in agreement with experimental findings of [93,165,178] as shown in Fig. 12, although the quantitative dependence remains to be fully validated.

The reason for the high dependence of reaction rate to turbulence appears to be connected primarily to the role of instabilities and their interaction with increased diffusivity. This has been shown in

Please cite this article as: S. Hochgreb, How fast can we burn, 2.0, Proceedings of the Combustion Institute, https://doi.org/10.1016/j.proci.2022.06.029

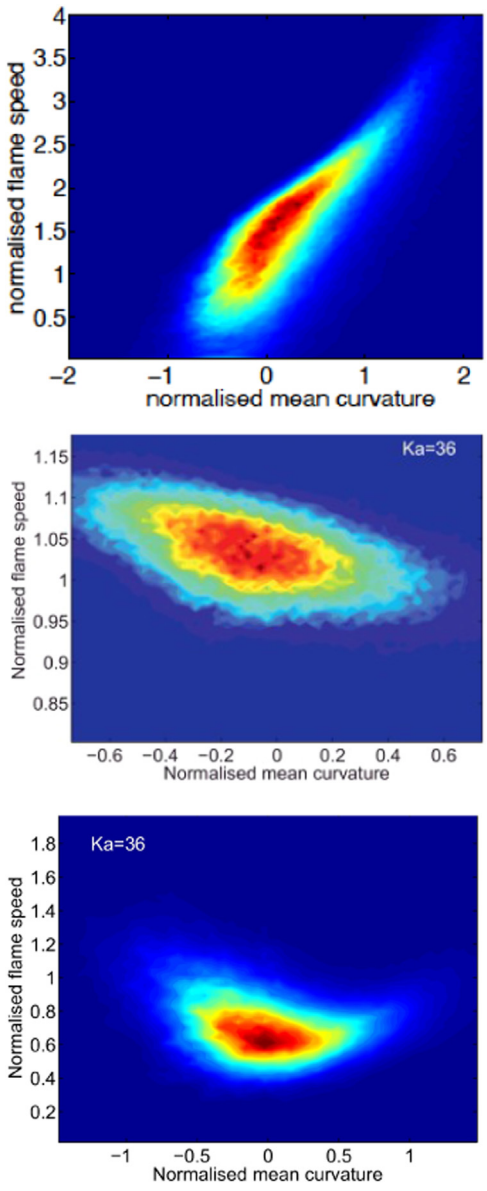

Fig. 16. Joint pdf of normalized reaction rate (as flame speed) as a function of curvature for simulations of H_2 (top), CH_4 (center) [181] and dodecane (bottom) [199], all for Ka = 36. Hydrogen: courtesy of A. Aspden, 2022.

various simulations where the Lewis number is artificially set to unity for comparison [198,200,203–205] (see also the blue dashed lines in Fig 14). A numerical demonstration of the higher sensitivity of flame propagation to curvature separately from tangential stretch is given for example in papers by [79,80]. Turbulence leads to regions of high curvature, which are unstable for low Le in the case of hydrogen, thus amplifying the growth of the flame area. Conversely, in the case of large fuel molecules, the low diffusivity leads to locally leaner regions, which suppress reaction. Fig. 16 shows the joint pdf of the normalised reaction rate and curvature: there is a clear correlation between curvature and reaction rate in the case of hydrogen, moderate in the case of methane, and a neutral one for dodecane. These remarkably different behaviors show how the microscale behavior of laminar flames are intimately connected to what kind of effect turbulence ultimately has on the rate of reaction, and whether and by how much turbulence can accelerate the latter or not.

A final note should be made with regards to the current flurry of studies, both experimental and numerical, on the behavior of hydrogen as potential energy carrier. Hydrogen is a particularly unusual fuel, which is sensitive to flow perturbations, leading to reaction throughout the low temperature region when flames are turbulent. Mizobuchi [97] showed very graphically how a vortex behaves in interaction with a rich hydrogen flame where oxygen is the deficient reactant, leading to extremely high reaction rates in the pre-flame zone. The investigations of Berger et al. [206], Altantzis et al. [80] and Howarth and Aspden [207] explore how the instabilities affect hydrogen combustion, and how these need to be incorporated into models, particularly in cases where the flames are unconditionally unstable. These interesting and marked effects suggest that there are still significant improvements to be made in models for the prediction of flames in mixtures with a variety of thermodiffusive characteristics.

7. Conclusions

In this brief review, we attempt to create a clear path between the understanding of the behavior of laminar flames under stretch and curvature, their measurement, and the broader consequences of their individual behavior as ensembles. The sensitivity of flames to perturbations in the flow field is intimately connected to differential molecular diffusion, leading to flame acceleration or suppression in larger scale turbulent flames. Therefore, understanding and properly measuring the behavior of laminar and turbulent flames requires a suitable understanding of how the different terms in the balance equations contribute to the evolution of the measureable quantities. This is particularly true in the case of turbulent flames, where some confusion remains in measurements of flame speeds and reaction rates, largely because of experimental difficulties, but also because of certain misconceptions about what the measurements should represent. Opportunities and recommendations follow from the discussion:

1. The definitions and interpretation of displacement and consumption speeds are both

Please cite this article as: S. Hochgreb, How fast can we burn, 2.0, Proceedings of the Combustion Institute, https://doi.org/10.1016/j.proci.2022.06.029

important and distinct, as they depend on the geometry of mean streamlines both in the laminar and turbulent case. Experimentalists should become well acquainted with these details of the quantities and how they can (and cannot) be isolated for comparisons with model.

2. There are significant opportunities to revisit some excellent previous measurements of turbulent premixed flames using modern high speed techniques over a wider range of conditions. The use of 2D and quasi-3D techniques for velocity measurements, combined with high resolution processing could yield valuable information regarding individual terms in the balance equations for a variety of flames, for well designed experiments.
3. The role of Lewis number in the evolution of turbulent flames is well explored in DNS, and there is a wealth of data of flame evolution of turbulent SEFs for a range of mixtures of different Lewis numbers which generally confirms the direction of flame behavior. However, the latter database is limited in experimental detail, even though selected models have been able to reproduce the final evolution of flame growth in various cases. There is an opportunity for better understanding the limits to the effect of turbulence on high (and low) Lewis number fuel mixtures, especially as new fuels are considered for a variety of applications.
4. The value of experimental measurements increases significantly when original measurements of flame position, flow velocity and their statistical properties can be preserved for revisiting for comparison with future models. In contrast, post-processed secondary variables which require assumptions or models in their derivation may not easily be re-usable.

As ever, the most valuable findings arise from detailed collaboration between modelers and experimenters. Bridging the language between these groups, and understanding what is both feasible and potentially useful will continue to require conversation and iteration.

Declaration of Competing Interest

The authors declare that they have no known competing financial interests or personal relationships that could have appeared to influence the work reported in this paper.

Acknowledgments

The University of Cambridge supported the author's time on this review. The author would like to acknowledge the help of Yutao Zheng in the compilation of turbulent flame data and many useful discussions. The author also benefited from many discussions with Andy J. Aspden, who also provided original plots for the present paper. Robert Barlow was kind enough to reading an early version of the manuscript and making many useful suggestions. I thank R. S. Cant for many discussions on turbulent flames, and with B. Renou and A. S. Tomboulides on laminar flames. The author is indebted to the many authors who wrote clear papers on the various difficult subjects, including D. Veynante and L. Vervisch on turbulent premixed flames, M. Matalon on instabilities, and G. K. Giannakopoulos and colleagues on laminar flame speeds. Finally, I am indebted to the additional reviewers of the paper, L. Vervisch, H. Pitsch, who provided useful suggestions, corrections, and criticisms, as well as A. Lipatnikov, for his legendary knowledge of Russian scientific literature on the topic. As ever, we benefit from standing on shoulders of giants. For the purpose of open access, the author has applied a Creative Commons Attribution (CC BY) licence to any Author Accepted Manuscript version arising from this submission.

References

[1] D. Bradley, How fast can we burn? Symp. (Int.) Combust. 24 (1) (1992) 247–262.
[2] T. Poinsot, D. Veynante, Theoretical and Numerical Combustion, CERFACS ELearning, 2012.
[3] A. Lipatnikov, Fundamentals of Premixed Turbulent Combustion, CRC Press, 2012.
[4] Turbulent Premixed Flames, N. Swaminathan, K.N.C. Bray (Eds.), Cambridge University Press, 2011.
[5] A. Lipatnikov, J. Chomiak, Effects of premixed flames on turbulence and turbulent scalar transport, Prog. Energy Combust. Sci. 36 (1) (2010) 1–102.
[6] B. Fiorina, D. Veynante, S. Candel, Modeling combustion chemistry in large eddy simulation of turbulent flames, Flow Turb. Combust. 94 (1) (2015) 3–42.
[7] D. Veynante, L. Vervisch, Turbulent combustion modeling, Prog. Energy Combust. Sci. 28 (3) (2002) 193–266.
[8] J.F. Driscoll, Turbulent premixed combustion: flamelet structure and its effect on turbulent burning velocities, Prog. Energy Combust. Sci. 34 (1) (2008) 91–134.
[9] J.F. Driscoll, J.H. Chen, A.W. Skiba, C.D. Carter, E.R. Hawkes, H. Wang, Premixed flames subjected to extreme turbulence: some questions and recent answers, Prog. Energy Combust. Sci. 76 (2020) 100802.
[10] B. Lewis, G. Von Elbe, Theory of flame propagation, in: Proceedings of the Symposium on Combustion, 1, Elsevier, 1948, pp. 183–188.
[11] E. Mallard, H.L. Le Chatelier, Sur la vitesse de propagation de la flamme, Ann. de Mines 8 (4) (1883) 274.

Please cite this article as: S. Hochgreb, How fast can we burn, 2.0, Proceedings of the Combustion Institute, https://doi.org/10.1016/j.proci.2022.06.029

[12] G. Damköhler, Der einfluss der turbulenz auf die flammengeschwindigkeit in gasgemischen, Zeitschrift für Elektrochemie und angewandte physikalische Chemie 46 (11) (1940) 601–626.
[13] A. Potnis, V.R. Unni, H.G. Im, A. Saha, Extinction of non-equidiffusive premixed flames with oscillating strain rates, Combust. Flame 234 (2021) 111617, doi:10.1016/j.combustflame.2021.111617.
[14] M.-E. Clavel, A. Vandel, V. Modica, Z. Chen, E. Varea, V. Moureau, B. Renou, Determination of spatially averaged consumption speed from spherical expanding flame: a new experimental methodology, Combust. Flame 235 (2022) 111720.
[15] G.K. Giannakopoulos, C.E. Frouzakis, S. Mohan, A.G. Tomboulides, M. Matalon, Consumption and displacement speeds of stretched premixed flames - theory and simulations, Combust. Flame 208 (2019) 164–181.
[16] F. Vance, Y. Shoshin, L. de Goey, J. van Oijen, A physical relationship between consumption and displacement speed for premixed flames with finite thickness, Proc. Combust. Inst. 38 (2) (2021) 2215–2223.
[17] Y. Mizobuchi, S. Tachibana, J. Shinio, S. Ogawa, T. Takeno, A numerical analysis of the structure of a turbulent hydrogen jet lifted flame, Proc. Combust. Inst. 29 (2) (2002) 2009–2015.
[18] E. Inanc, A. Kempf, N. Chakraborty, Scalar gradient and flame propagation statistics of a flame-resolved laboratory-scale turbulent stratified burner simulation, Combust. Flame 238 (2022) 111917.
[19] V. Moureau, P. Domingo, L. Vervisch, From large-eddy simulation to direct numerical simulation of a lean premixed swirl flame: filtered laminar flame-pdf modeling, Combust. Flame 158 (7) (2011) 1340–1357.
[20] S.B. Pope, Small scales, many species and the manifold challenges of turbulent combustion, Proc. Combust. Inst. 34 (1) (2013) 1–31.
[21] A.N. Lipatnikov, Stratified turbulent flames: recent advances in understanding the influence of mixture inhomogeneities on premixed combustion and modeling challenges, Prog. Energy Combust. Sci. 62 (2017) 87–132.
[22] S. Hochgreb, Mind the gap: turbulent combustion model validation and future needs, Proc. Combust. Inst. 37 (2) (2019) 2091–2107.
[23] A. Masri, Challenges for turbulent combustion, Proc. Combust. Inst. 38 (1) (2021) 121–155.
[24] A.M. Steinberg, P.E. Hamlington, X. Zhao, Structure and dynamics of highly turbulent premixed combustion, Prog. Energy Combust. Sci. 85 (2021) 100900.
[25] J. van Oijen, A. Donini, R. Bastiaans, J. ten Thije Boonkkamp, L. de Goey, State-of-the-art in premixed combustion modeling using flamelet generated manifolds, Prog. Energy Combust. Sci. 57 (2016) 30–74.
[26] S. Pope, The evolution of surfaces in turbulence, Int. J. Eng. Sci. 26 (5) (1988) 445–469.
[27] F. Egolfopoulos, N. Hansen, Y. Ju, K. Kohse-Höinghaus, C. Law, F. Qi, Advances and challenges in laminar flame experiments and implications for combustion chemistry, Prog. Energy Combust. Sci. 43 (2014) 36–67.
[28] A.A. Konnov, A. Mohammad, V.R. Kishore, N.I. Kim, C. Prathap, S. Kumar, A comprehensive review of measurements and data analysis of laminar burning velocities for various fuel+air mixtures, Prog. Energy Combust. Sci. 68 (2018) 197–267.
[29] J.T. Farrell, R. Johnston, I. Androulakis, Molecular structure effects on laminar burning velocities at elevated temperature and pressure, SAE Trans. (2004) 1404–1425.
[30] D. Bradley, M. Lawes, K. Liu, M.S. Mansour, Measurements and correlations of turbulent burning velocities over wide ranges of fuels and elevated pressures, Proc. Combust. Inst. 34 (1) (2013) 1519–1526.
[31] D. Bradley, R. Hicks, M. Lawes, C. Sheppard, R. Woolley, The measurement of laminar burning velocities and markstein numbers for iso-octane–air and isooctane–n-heptane–air mixtures at elevated temperatures and pressures in an explosion bomb, Combust. Flame 115 (1) (1998) 126–144.
[32] D. Bradley, M. Lawes, M. Morsy, Flame speed and particle image velocimetry measurements of laminar burning velocities and markstein numbers of some hydrocarbons, Fuel 243 (2019) 423–432.
[33] D. Bradley, M. Lawes, K. Liu, S. Verhelst, R. Woolley, Laminar burning velocities of lean hydrogen-air mixtures at pressures up to 1.0 mpa, Combust. Flame 149 (1–2) (2007) 162–172.
[34] F. Egolfopoulos, C. Law, An experimental and computational study of the burning rates of ultra-lean to moderately-rich H2/O2/N2 laminar flames with pressure variations, Proc. Combust. Inst. 23 (1990) 333–340.
[35] C. Xiouris, T. Ye, J. Jayachandran, F. Egolfopoulos, Laminar flame speeds under engine-relevant conditions: uncertainty quantification and minimization in spherically expanding flame experiments, Combust. Flame 163 (2016) 270–283.
[36] C. Law, C. Sung, Structure, aerodynamics, and geometry of premixed flamelets, Prog. Energy Combust. Sci. 26 (4) (2000) 459–505.
[37] S. Tse, D. Zhu, C. Law, Morphology and burning rates of expanding spherical flames in H2/O2/inert mixtures up to 60 atmospheres, Proc. Combust. Inst. 28 (2) (2000) 1793–1800.
[38] M. Mehl, W.J. Pitz, C.K. Westbrook, H.J. Curran, Kinetic modeling of gasoline surrogate components and mixtures under engine conditions, Proc. Combust. Inst. 33 (1) (2011) 193–200.
[39] F. Halter, C. Chauveau, I. Gökalp, Characterization of the effects of hydrogen addition in premixed methane/air flames, Int. J. Hydrogen Energy 32 (13) (2007) 2585–2592.
[40] H. Kobayashi, A. Hayakawa, K.K.A. Somarathne, E.C. Okafor, Science and technology of ammonia combustion, Proc. Combust. Inst. 37 (1) (2019) 109–133.
[41] Y. Zhang, M. Jeanson, R. Mével, Z. Chen, N. Chaumeix, Tailored mixture properties for accurate laminar flame speed measurement from spherically expanding flames: application to h2/o2/n2/he mixtures, Combust. Flame 231 (2021) 111487.
[42] R. Grosseuvres, A. Comandini, A. Bentaib, N. Chaumeix, Combustion properties of H2/N2/O2/steam mixtures, Proc. Combust. Inst. 37 (2) (2019) 1537–1546.

Please cite this article as: S. Hochgreb, How fast can we burn, 2.0, Proceedings of the Combustion Institute, https://doi.org/10.1016/j.proci.2022.06.029

[43] J. Beeckmann, R. Hesse, J. Schaback, H. Pitsch, E. Varea, N. Chaumeix, Flame propagation speed and markstein length of spherically expanding flames: assessment of extrapolation and measurement techniques, Proc. Combust. Inst. 37 (2) (2019) 1521–1528.
[44] F. Halter, C. Chauveau, N. Djebaili-Chaumeix, I. Gökalp, Characterization of the effects of pressure and hydrogen concentration on laminar burning velocities of methane-hydrogen-air mixtures, Proc. Combust. Inst. 30 (1) (2005) 201–208.
[45] E. Okafor, Y. Nagano, T. Kitagawa, Experimental and theoretical analysis of cellular instability in lean H2-Ch4-air flames at elevated pressures, Int. J. Hydrogen Energy 41 (15) (2016) 6581–6592.
[46] N. Bouvet, F. Halter, C. Chauveau, Y. Yoon, On the effective lewis number formulations for lean hydrogen/hydrocarbon/air mixtures, Int. J. Hydrogen Energy 38 (14) (2013) 5949–5960.
[47] T. Shu, Y. Xue, Z. Zhou, Z. Ren, An experimental study of laminar ammonia/methane/air premixed flames using expanding spherical flames, Fuel 290 (2021) 120003.
[48] B. Mei, J. Zhang, X. Shi, Z. Xi, Y. Li, Enhancement of ammonia combustion with partial fuel cracking strategy: laminar flame propagation and kinetic modeling investigation of nh3/h2/n2/air mixtures up to 10 atm, Combust. Flame 231 (2021) 111472.
[49] A. Ichikawa, A. Hayakawa, Y. Kitagawa, K. Somarathne, Laminar burning velocity and markstein length of ammonia/hydrogen/air premixed flames at elevated pressures, Int. J. Hydrogen Energy 40 (30) (2015) 9570–9578.
[50] X. Han, Z. Wang, Y. He, Y. Zhu, K. Cen, Experimental and kinetic modeling study of laminar burning velocities of NH3/syngas/air premixed flames, Combust. Flame 213 (2020) 1–13.
[51] K.P. Shrestha, C. Lhuillier, A.A. Barbosa, P. Brequigny, F. Contino, C. Mounaïm-Rousselle, L. Seidel, F. Mauss, An experimental and modeling study of ammonia with enriched oxygen content and ammonia/hydrogen laminar flame speed at elevated pressure and temperature, Proc. Combust. Inst. 38 (2) (2021) 2163–2174.
[52] G.J. Gotama, A. Hayakawa, E.C. Okafor, R. Kanoshima, M. Hayashi, T. Kudo, H. Kobayashi, Measurement of the laminar burning velocity and kinetics study of the importance of the hydrogen recovery mechanism of ammonia/hydrogen/air premixed flames, Combust. Flame 236 (2022) 111753.
[53] H. Tang, C. Yang, G. Wang, T.F. Guiberti, G. Magnotti, Raman spectroscopy for quantitative measurements of temperature and major species in high-pressure non-premixed NH3/H2/N2 counterflow flames, Combust. Flame 237 (2022) 111840.
[54] S. Jerzembeck, N. Peters, P. Pepiot-Desjardins, H. Pitsch, Laminar burning velocities at high pressure for primary reference fuels and gasoline: experimental and numerical investigation, Combust. Flame 156 (2) (2009) 292–301.
[55] S.M. Candel, T.J. Poinsot, Flame stretch and the balance equation for the flame area, Combus. Sci. Technol. 70 (1 - 3) (1990) 1–15.
[56] C. Wu, C. Law, On the determination of laminar flame speeds from stretched flames, Symp. (Int.) Combust. 20 (1) (1985) 1941–1949. Twentieth Symposium (International) on Combustion
[57] C. Law, D. Zhu, G. Yu, Propagation and extinction of stretched premixed flames, Symp. (Int.) Combust. 21 (1) (1988) 1419–1426.
[58] C.M. Vagelopoulos, F.N. Egolfopoulos, Direct experimental determination of laminar flame speeds, Symp. (Int.) Combust. 27 (1) (1998) 513–519.
[59] C. Vagelopoulos, F. Egolfopoulos, C. Law, Further considerations on the determination of laminar flame speeds with the counterflow twin-flame technique, Symp. (Int.) Combust. 25 (1) (1994) 1341–1347.
[60] B. Karlovitz, D.W. Denniston, H.D. Knapschaefer, F.E. Wells, Studies on turbulent flames, in: Fourth Symposium (Intl) on Combustion, 1953, pp. 613–620.
[61] Y.B. Zeldovich, G.I. Barenblatt, V.B. Librovich, G.M. Makhaviladze, The mathematical theory of combustion and explosions, Consultants Bureau, 1985.
[62] G.H. Markstein, Experimental and theoretical studies of flame front stability, J. Aeronaut. Sci. 18 (1951) 199–209.
[63] J. Tien, M. Matalon, On the burning velocity of stretched flames, Combust. Flame 84 (3) (1991) 238–248.
[64] J. Jayachandran, R. Zhao, F.N. Egolfopoulos, Determination of laminar flame speeds using stagnation and spherically expanding flames: molecular transport and radiation effects, Combust. Flame 161 (9) (2014) 2305–2316.
[65] S.G. Davis, C. Law, Determination of and fuel structure effects on laminar flame speeds of C1 to C8 hydrocarbons, Combust. Sci. Technol. 140 (1–6) (1998) 427–449.
[66] G.K. Giannakopoulos, A. Gatzoulis, C.E. Frouzakis, M. Matalon, A.G. Tomboulides, Consistent definitions of "flame displacement speed" and "Markstein length" for premixed flame propagation, Combust. Flame 162 (4) (2015) 1249–1264.
[67] A. Kelley, C. Law, Nonlinear effects in the extraction of laminar flame speeds from expanding spherical flames, Combust. Flame 156 (9) (2009) 1844–1851.
[68] J. van Oijen, R. Bastiaans, L. de Goey, Low-dimensional manifolds in direct numerical simulations of premixed turbulent flames, Proc. Combust. Inst. 31 (1) (2007) 1377–1384.
[69] A. Vreman, B. Albrecht, J. van Oijen, L. de Goey, R. Bastiaans, Premixed and nonpremixed generated manifolds in large-Eddy simulation of Sandia flame D and F, Combust. Flame 153 (3) (2008) 394–416.
[70] B. Fiorina, O. Gicquel, L. Vervisch, S. Carpentier, N. Darabiha, Approximating the chemical structure of partially premixed and diffusion counterflow flames using fpi flamelet tabulation, Combust. Flame 140 (3) (2005) 147–160.
[71] O. Gicquel, N. Darabiha, D. Thévenin, Laminar premixed hydrogen/air counterflow flame simulations using flame prolongation of ILDM with differential diffusion, Proc. Combust. Inst. 28 (2) (2000) 1901–1908.
[72] X. Wen, S. Hartl, A. Dreizler, J. Janicka, C. Hasse, Flame structure analysis of turbulent premixed/stratified flames with H2 addition con-

Please cite this article as: S. Hochgreb, How fast can we burn, 2.0, Proceedings of the Combustion Institute, https://doi.org/10.1016/j.proci.2022.06.029

sidering differential diffusion and stretch effects, Proc. Combust. Inst. 38 (2) (2021) 2993–3001.
[73] E. Knudsen, H. Kolla, E.R. Hawkes, H. Pitsch, Les of a premixed jet flame dns using a strained flamelet model, Combust. Flame 160 (12) (2013) 2911–2927.
[74] L. de Goey, J. ten Thije Boonkkamp, A flamelet description of premixed laminar flames and the relation with flame stretch, Combust. Flame 119 (3) (1999) 253–271.
[75] J. de Swart, G. Groot, J. van Oijen, J. ten Thije Boonkkamp, L. de Goey, Detailed analysis of the mass burning rate of stretched flames including preferential diffusion effects, Combust. Flame 145 (1) (2006) 245–258.
[76] B. Fiorina, R. Mercier, G. Kuenne, A. Ketelheun, A. Avdić, J. Janicka, D. Geyer, A. Dreizler, E. Alenius, C. Duwig, P. Trisjono, K. Kleinheinz, S. Kang, H. Pitsch, F. Proch, F.C. Marincola, A. Kempf, Challenging modeling strategies for LES of non-adiabatic turbulent stratified combustion, Combust. Flame 162 (11) (2015) 4264–4282.
[77] A.M. Klimov, Prickle. mekh. i. tech. fiz., Laminarnoe playa v turbulento potoke (Laminar Flames in Turbulent Flows) 3 (1963) 49.
[78] S. Nambully, P. Domingo, V. Moureau, L. Vervisch, A filtered-laminar-flame pdf sub-grid scale closure for LES of premixed turbulent flames. Part I: formalism and application to a bluff-body burner with differential diffusion, Combust. Flame 161 (7) (2014) 1756–1774.
[79] F. Thiesset, F. Halter, C. Bariki, C. Lapeyre, C. Chauveau, I. Gökalp, L. Selle, T. Poinsot, Isolating strain and curvature effects in premixed flame/vortex interactions, J. Fluid Mech. 831 (2017) 618–654.
[80] C. Altantzis, C.E. Frouzakis, A.G. Tomboulides, M. Matalon, K. Boulouchos, Hydrodynamic and thermodiffusive instability effects on the evolution of laminar planar lean premixed hydrogen flames, J. Fluid Mech. 700 (2012) 329–361.
[81] D.R. Dowdy, D.B. Smith, S.C. Taylor, A. Williams, The use of expanding spherical flames to determine burning velocities and stretch effects in hydrogen/air mixtures, Symp. (Int.) Combust. 23 (1) (1991) 325–332.
[82] M.L. Frankel, G.I. Sivanshinsky, On quenching of curved flames, Combust. Sci. Technol. 40 (5–6) (1984) 257–268.
[83] P.D. Ronney, G.I. Sivashinsky, A theoretical study of propagation and extinction of nonsteady spherical flame fronts, SIAM J. Appl. Math. 49 (4) (1989) 1029–1046.
[84] E. Varea, V. Modica, A. Vandel, B. Renou, Measurement of laminar burning velocity and markstein length relative to fresh gases using a new postprocessing procedure: application to laminar spherical flames for methane, ethanol and isooctane/air mixtures, Combust. Flame 159 (2) (2012) 577–590.
[85] F. Wu, W. Liang, Z. Chen, Y. Ju, C.K. Law, Uncertainty in stretch extrapolation of laminar flame speed from expanding spherical flames, Proc. Combust. Inst. 35 (1) (2015) 663–670.
[86] F. Halter, T. Tahtouh, C. Mounaïm-Rousselle, Nonlinear effects of stretch on the flame front propagation, Combust. Flame 157 (10) (2010) 1825–1832.
[87] A. Lefebvre, H. Larabi, V. Moureau, G. Lartigue, E. Varea, V. Modica, B. Renou, Formalism for spatially averaged consumption speed considering spherically expanding flame configuration, Combust. Flame 173 (2016) 235–244.
[88] G. Darrieus, Propagation d'un front de flamme, 1945. La Technique Moderne (Paris) and in 1945 at Congrès de Mécanique Appliquée.
[89] L.D. Landau, On the theory of slow combustion, Acta Physicochim. USSR 19 (77) (1944).
[90] G.I. Sivashinsky, C.K. Law, G. Joulin, On stability of premixed flames in stagnation – point flow, Combust. Sci. Technol. 28 (3–4) (1982) 155–159.
[91] O. Kwon, G. Rozenchan, C. Law, Cellular instabilities and self-acceleration of outwardly propagating spherical flames, Proc. Combust. Inst. 29 (2) (2002) 1775–1783.
[92] Z.-Y. Sun, F.-S. Liu, X.-C. Bao, X.-H. Liu, Research on cellular instabilities in outwardly propagating spherical hydrogen-air flames, Int. J. Hydrogen Energy 37 (9) (2012) 7889–7899.
[93] D. Bradley, Instabilities and flame speeds in large-scale premixed gaseous explosions, Philos. Trans. R. Soc. A 358 (1764) (2000) 3567–3581.
[94] D. Bradley, M. Lawes, M. Mansour, Explosion bomb measurements of ethanol-air laminar gaseous flame characteristics at pressures up to 1.4 mpa, Combust. Flame 156 (7) (2009) 1462–1470.
[95] H. Kobayashi, H. Kawazoe, Flame instability effects on the smallest wrinkling scale and burning velocity of high-pressure turbulent premixed flames, Proc. Combust. Inst. 28 (1) (2000) 375–382.
[96] F. Creta, P. Lapenna, R. Lamioni, N. Fogla, M. Matalon, Propagation of premixed flames in the presence of Darrieus–Landau and thermal diffusive instabilities, Combust. Flame 216 (2020) 256–270.
[97] Y. Mizobuchi, Large deformation effects on the combustion structure of a hydrogen/air rich premixed flame, Combust. Flame (2021) 111732.
[98] P. Clavin, G. Searby, Combustion Waves and Fronts in Flows, Cambridge University Press, 2016.
[99] M. Matalon, The Darrieus–Landau instability of premixed flames, Fluid Dyn. Res. 50 (2018) 051412.
[100] M. Matalon, C. Cui, J.K. Bechtold, Hydrodynamic theory of premixed flames: effects of stoichiometry, variable transport coefficients and arbitrary reaction orders, J. Fluid Mech. 487 (2003) 179–210, doi:10.1017/S0022112003004683.
[101] M. Matalon, B.J. Matkowsky, Flames as gasdynamic discontinuities, J. Fluid Mech. 124 (1982) 239–259.
[102] F. Creta, M. Matalon, Strain rate effects on the nonlinear development of hydrodynamically unstable flames, Proc. Combust. Inst. 33 (1) (2011) 1087–1094.
[103] G.H. Markstein, Nonsteady Flame Propagation, AGARDograph, 75, Elsevier, 1964.
[104] J. Bechtold, M. Matalon, Hydrodynamic and diffusion effects on the stability of spherically expanding flames, Combust. Flame 67 (1) (1987) 77–90.
[105] R. Addabbo, J. Bechtold, M. Matalon, Wrinkling of spherically expanding flames, Proc. Combust. Inst. 29 (2) (2002) 1527–1535.
[106] G. Jomaas, C.K. Law, J.K. Bechtold, On transition to cellularity in expanding spherical flames, J. Fluid Mech. 583 (2007) 1–26.

Please cite this article as: S. Hochgreb, How fast can we burn, 2.0, Proceedings of the Combustion Institute, https://doi.org/10.1016/j.proci.2022.06.029

[107] L. Gillespie, M. Lawes, C.G.W. Sheppard, R. Woolley, Aspects of laminar and turbulent burning velocity relevant to SI engines, SAE Trans. Sect. 3 109 (2000) 13–33.
[108] S. Yang, A. Saha, Z. Liu, C.K. Law, Role of Darrieus–Landau instability in propagation of expanding turbulent flames, J. Fluid Mech. 850 (2018) 784–802.
[109] P. Lapenna, R. Lamioni, F. Creta, Subgrid modeling of intrinsic instabilities in premixed flame propagation, Proc. Combust. Inst. 38 (2) (2021) 2001–2011.
[110] G. Troiani, F. Creta, M. Matalon, Experimental investigation of darrieus–landau instability effects on turbulent premixed flames, Proc. Combust. Inst. 35 (2) (2015) 1451–1459.
[111] C.E. Frouzakis, N. Fogla, A.G. Tomboulides, C. Altantzis, M. Matalon, Numerical study of unstable hydrogen/air flames: shape and propagation speed, Proc. Combust. Inst. 35 (1) (2015) 1087–1095.
[112] N. Fogla, F. Creta, M. Matalon, The turbulent flame speed for low-to-moderate turbulence intensities: hydrodynamic theory vs. experiments, Combust. Flame 175 (2017) 155–169.
[113] N. Fogla, F. Creta, M. Matalon, Effect of folds and pockets on the topology and propagation of premixed turbulent flames, Combust. Flame 162 (7) (2015) 2758–2777.
[114] S. Kadowaki, T. Hasegawa, Numerical simulation of dynamics of premixed flames: flame instability and vortex–flame interaction, Prog. Energy Combust. Sci. 31 (3) (2005) 193–241.
[115] N. Peters, Turbulent Combustion, Cambridge University Press, 2000.
[116] A. Lipatnikov, J. Chomiak, Molecular transport effects on turbulent flame propagation and structure, Prog. Energy Combust. Sci. 31 (1) (2005) 1–73.
[117] A. Lipatnikov, W. Li, L. Jiang, S. Shy, Does density ratio significantly affect turbulent flame speed? Flow Turb. Combust. 98 (4) (2017) 1153–1172.
[118] V. Sabelnikov, A. Lipatnikov, Recent advances in understanding of thermal expansion effects in premixed turbulent flames, Annu. Rev. Fluid Mech. 49 (2017) 91–117.
[119] A. Masri, R. Bilger, Turbulent diffusion flames of hydrocarbon fuels stabilized on a bluff body, Symp. (Int.) Combust. 20 (1) (1985) 319–326.
[120] L. Gicquel, G. Staffelbach, T. Poinsot, Large eddy simulations of gaseous flames in gas turbine combustion chambers, Prog. Energy Combust. Sci. 38 (6) (2012) 782–817.
[121] H. Pitsch, Large-eddy simulation of turbulent combustion, Annu. Rev. Fluid Mech. 38 (1) (2006) 453–482.
[122] J.F. Driscoll, Turbulent premixed combustion: flamelet structure and its effect on turbulent burning velocities, Prog. Energy Combust. Sci. 34 (1) (2008) 91–134.
[123] H. Kobayashi, T. Tamura, K. Maruta, T. Niioka, F.A. Williams, Burning velocity of turbulent premixed flames in a high-pressure environment, in: Symposium (International) on Combustion, 26, 1996, pp. 389–396.
[124] H. Kobayashi, Experimental study of high-pressure turbulent premixed flames, Exp. Therm Fluid Sci. 26 (2–4) (2002) 375–387.
[125] P. Tamadonfar, Ö.L. Gülder, Effects of mixture composition and turbulence intensity on flame front structure and burning velocities of premixed turbulent hydrocarbon/air bunsen flames, Combust. Flame 162 (12) (2015) 4417–4441.
[126] T.M. Wabel, A.W. Skiba, J.F. Driscoll, Turbulent burning velocity measurements: extended to extreme levels of turbulence, Proc. Combust. Inst. 36 (2) (2017) 1801–1808.
[127] M. Wu, S. Kwon, J. Driscoll, G. Faeth, Turbulent premixed hydrogen/air flames at high Reynolds numbers, Combust. Sci. Technol. 73 (1–3) (1990) 327–350.
[128] P. Venkateswaran, A.D. Marshall, D.R. Noble, J. Antezana, J.M. Seitzman, T.C. Lieuwen, Global turbulent consumption speeds of H_2/CO blends, in: ASME Turbo Expo 2009: Power for Land, Sea, and Air, American Society of Mechanical Engineers Digital Collection, 2009, pp. 559–570.
[129] K. Bray, P.A. Libby, J. Moss, Unified modeling approach for premixed turbulent combustion—part I: general formulation, Combust. Flame 61 (1) (1985) 87–102.
[130] L. Kostiuk, K. Bray, R. Cheng, Experimental study of premixed turbulent combustion in opposed streams. Part II—reacting flow field and extinction, Combust. Flame 92 (4) (1993) 396–409.
[131] R.S.C. Margolis, K.N.C. Bray, L.W. Kostiuk, B. Rogg, Flow divergence effects in strained laminar flamelets for premixed turbulent combustion, Combust. Sci. Technol. 95 (1–6) (1993) 261–276.
[132] I. Shepherd, R. Cheng, The burning rate of premixed flames in moderate and intense turbulence, Combust. Flame 127 (3) (2001) 2066–2075.
[133] R. Cheng, I. Shepherd, The influence of burner geometry on premixed turbulent flame propagation, Combust. Flame 85 (1) (1991) 7–26.
[134] R. Cheng, I. Shepherd, L. Talbot, Reaction rates in premixed turbulent flames and their relevance to the turbulent burning speed, in: Symposium (International) on Combustion, 22, Elsevier, 1989, pp. 771–780.
[135] I. Shepherd, E. Bourguignon, Y. Michou, I. Gökalp, The burning rate in turbulent Bunsen flames, in: Symposium (International) on Combustion, 27, Elsevier, 1998, pp. 909–916.
[136] H. Kobayashi, K. Seyama, H. Hagiwara, Y. Ogami, Burning velocity correlation of methane/air turbulent premixed flames at high pressure and high temperature, Proc. Combust. Inst. 30 (1) (2005) 827–834.
[137] S.A. Filatyev, J.F. Driscoll, C.D. Carter, J.M. Donbar, Measured properties of turbulent premixed flames for model assessment, including burning velocities, stretch rates, and surface densities, Combust. Flame 141 (1–2) (2005) 1–21.
[138] F.T. Yuen, Ö.L. Gülder, Premixed turbulent flame front structure investigation by Rayleigh scattering in the thin reaction zone regime, Proc. Combust. Inst. 32 (2) (2009) 1747–1754.
[139] F.T. Yuen, Ö.L. Gülder, Investigation of dynamics of lean turbulent premixed flames by Rayleigh scattering, AIAA J. 47 (12) (2009) 2964–2973.
[140] F.T. Yuen, Ö.L. Gülder, Turbulent premixed flame front dynamics and implications for limits of

Please cite this article as: S. Hochgreb, How fast can we burn, 2.0, Proceedings of the Combustion Institute, https://doi.org/10.1016/j.proci.2022.06.029

flamelet hypothesis, Proc. Combust. Inst. 34 (1) (2013) 1393–1400.
[141] G. Troiani, F. Battista, F. Picano, Turbulent consumption speed via local dilatation rate measurements in a premixed Bunsen jet, Combust. Flame 160 (10) (2013) 2029–2037.
[142] P. Tamadonfar, Ö.L. Gülder, Flame brush characteristics and burning velocities of premixed turbulent methane/air bunsen flames, Combust. Flame 161 (12) (2014) 3154–3165.
[143] P. Tamadonfar, Ö.L. Gülder, Effect of burner diameter on the burning velocity of premixed turbulent flames stabilized on bunsen-type burners, Exp. Therm Fluid Sci. 73 (2016) 42–48.
[144] R. Abdel-Gayed, K. Al-Khishali, D. Bradley, Turbulent burning velocities and flame straining in explosions, Proc. R. Soc. Lond. A 391 (1801) (1984) 393–414.
[145] C. Liu, S. Shy, H. Chen, M. Peng, On interaction of centrally-ignited, outwardly-propagating premixed flames with fully-developed isotropic turbulence at elevated pressure, Proc. Combust. Inst. 33 (1) (2011) 1293–1299.
[146] S. Chaudhuri, F. Wu, D. Zhu, C.K. Law, Flame speed and self-similar propagation of expanding turbulent premixed flames, Phys. Rev. Lett. 108 (4) (2012) 044503.
[147] S. Chaudhuri, F. Wu, C.K. Law, Scaling of turbulent flame speed for expanding flames with Markstein diffusion considerations, Phys. Rev. E 88 (3) (2013) 033005.
[148] S. Chaudhuri, A. Saha, C.K. Law, On flame–turbulence interaction in constant-pressure expanding flames, Proc. Combust. Inst. 35 (2) (2015) 1331–1339.
[149] L. Jiang, S. Shy, W. Li, H. Huang, M. Nguyen, High-temperature, high-pressure burning velocities of expanding turbulent premixed flames and their comparison with bunsen-type flames, Combust. Flame 172 (2016) 173–182.
[150] A. Lipatnikov, J. Chomiak, Turbulent flame speed and thickness: phenomenology, evaluation, and application in multi-dimensional simulations, Prog. Energy Combust. Sci. 28 (1) (2002) 1–74.
[151] D. Bradley, A.K.C. Lau, M. Lawes, F.T. Smith, Flame stretch rate as a determinant of turbulent burning velocity, Philos. Trans. R. Soc. Lond. Ser. A 338 (1650) (1992) 359–387.
[152] A.N. Lipatnikov, J. Chomiak, Application of the markstein number concept to curved turbulent flames, Combust. Sci. Technol. 176 (3) (2004) 331–358.
[153] P. Venkateswaran, A. Marshall, J. Seitzman, T. Lieuwen, Scaling turbulent flame speeds of negative markstein length fuel blends using leading points concepts, Combust. Flame 162 (2) (2015) 375–387.
[154] S. Daniele, P. Jansohn, J. Mantzaras, K. Boulouchos, Turbulent flame speed for syngas at gas turbine relevant conditions, Proc. Combust. Inst. 33 (2) (2011) 2937–2944.
[155] F. Hernández-Pérez, F. Yuen, C. Groth, Ö. Gülder, LES of a laboratory-scale turbulent premixed bunsen flame using FSD, PCM-FPI and thickened flame models, Proc. Combust. Inst. 33 (1) (2011) 1365–1371.
[156] Y. Shoraka, S. Galindo-Lopez, M. Cleary, A. Masri, F. Salehi, A. Klimenko, Modelling of a turbulent premixed flame series using a new MMC-LES model with a shadow position reference variable, Proc. Combust. Inst. (2020).
[157] A.M. Steinberg, J.F. Driscoll, N. Swaminathan, Statistics and dynamics of turbulence–flame alignment in premixed combustion, Combust. Flame 159 (8) (2012) 2576–2588.
[158] B. Renou, A. Mura, E. Samson, A. Boukhalfa, Characterization of the local flame structure and the flame surface density for freely propagating premixed flames at various lewis numbers, Combust. Sci. Technol. 174 (4) (2002) 143–179.
[159] D. Bradley, M. Haq, R. Hicks, T. Kitagawa, M. Lawes, C. Sheppard, R. Woolley, Turbulent burning velocity, burned gas distribution, and associated flame surface definition, Combust. Flame 133 (4) (2003) 415–430.
[160] D. Bradley, M. Lawes, M. Mansour, Correlation of turbulent burning velocities of ethanol–air, measured in a fan-stirred bomb up to 1.2 MPa, Combust. Flame 158 (1) (2011) 123–138.
[161] S. Chaudhuri, V. Akkerman, C.K. Law, Spectral formulation of turbulent flame speed with consideration of hydrodynamic instability, Phys. Rev. E 84 (2) (2011) 026322.
[162] I.A.G. Gostintsev Yu. A., Y.V. Shulerin, Self-similar propagation of a free turbulent flame in mixed gas mixtures, Combust. Explos. Shock 24 (1988) 563.
[163] A. Lipatnikov, J. Chomiak, Turbulent burning velocity and speed of developing, curved, and strained flames, Proc. Combust. Inst. 29 (2) (2002) 2113–2121.
[164] I. Ahmed, N. Swaminathan, Simulation of spherically expanding turbulent premixed flames, Combust. Sci. Technol. 185 (10) (2013) 1509–1540.
[165] M. Nguyen, D. Yu, S. Shy, General correlations of high pressure turbulent burning velocities with the consideration of Lewis number effect, Proc. Combust. Inst. 37 (2) (2019) 2391–2398.
[166] S. Chaudhuri, A. Saha, C.K. Law, On flame–turbulence interaction in constant-pressure expanding flames, Proc. Combust. Inst. 35 (2) (2015) 1331–1339.
[167] H. Wang, E. Hawkes, J. Chen, B. Zhou, Z. Li, M. Aldén, Direct numerical simulations of a high Karlovitz number laboratory premixed jet flame - an analysis of flame stretch and flame thickening, J. Fluid Mech. 815 (2017) 511–536.
[168] J. Hult, S. Gashi, N. Chakraborty, M. Klein, K.W. Jenkins, S. Cant, C.F. Kaminski, Measurement of flame surface density for turbulent premixed flames using PLIF and DNS, Proc. Combust. Inst. 31 (1) (2007) 1319–1326.
[169] V. Karpov, E. Severin, Effects of molecular-transport coefficients on the rate of turbulent combustion, Combust. Explos. Shock Waves (1980).
[170] H. Kido, S. Huang, K. Tanoue, T. Nitta, Improvement of lean hydrocarbon mixtures combustion performance by hydrogen addition and its mechanisms, in: Proceedings Comodia 94 Symposium, p119, 124, 1994.
[171] M. Nakahara, H. Kido, A study of the premixed turbulent combustion mechanism taking the prefer-

Please cite this article as: S. Hochgreb, How fast can we burn, 2.0, Proceedings of the Combustion Institute, https://doi.org/10.1016/j.proci.2022.06.029

ential diffusion effect into consideration, Mem. Fac. Eng, Kyushu Univ. 58 (82-82) (1998).
[172] H. Kido, M. Nakahara, A model of turbulent burning velocity taking the preferential diffusion effect into consideration, JSME Int. J. Ser. B Fluids Therm. Eng. 41 (3) (1998) 666–673.
[173] Burning velocities, markstein lengths, and flame quenching for spherical methane-air flames: a computational study, Combust. Flame 104 (1) (1996) 176–198.
[174] M. Nguyen, D. Yu, C. Chen, S. Shy, General correlations of iso-octane turbulent burning velocities relevant to spark ignition engines, Energies 12 (10) (2019).
[175] V. Karpov, A. Lipatnikov, V. imont, A test of an engineering model of premixed turbulent combustion, Symp. (Int.) Combust. 26 (1) (1996) 249–257.
[176] V.R. Kuznetsov, V.A. Sabel'nikov, Turbulence and Combustion, Hemisphere Publishing Corp., New York, 1990.
[177] S. Muppala, M. Nakahara, N. Aluri, H. Kido, J. Wen, M. Papalexandris, Experimental and analytical investigation of the turbulent burning velocity of two-component fuel mixtures of hydrogen, methane and propane, Int. J. Hydrogen Energy 34 (22) (2009) 9258–9265.
[178] P. Ahmed, B. Thorne, M. Lawes, S. Hochgreb, G.V. Nivarti, R.S. Cant, Three dimensional measurements of surface areas and burning velocities of turbulent spherical flames, Combust. Flame 233 (2021) 111586.
[179] D. Veynante, G. Lodato, P. Domingo, L. Vervisch, E.R. Hawkes, Estimation of three-dimensional flame surface densities from planar images in turbulent premixed combustion, Exp Fluids 49 (1) (2010) 267–278.
[180] Y. Zheng, L. Weller, S. Hochgreb, 3D surface density measurements via orthogonal cross-planar Mie scattering in a low-turbulence Bunsen flame, Proc. Comb. Inst. (2022). accepted, in press. https://authors.elsevier.com/tracking/article/details.do?aid=4752&jid=PROCI&surname=Zheng.
[181] A. Aspden, M. Day, J. Bell, Three-dimensional direct numerical simulation of turbulent lean premixed methane combustion with detailed kinetics, Combust. Flame 166 (2016) 266–283.
[182] N. Chakraborty, D. Alwazzan, M. Klein, R. Cant, On the validity of damköhler's first hypothesis in turbulent bunsen burner flames: a computational analysis, Proc. Combust. Inst. 37 (2) (2019) 2231–2239.
[183] O. Colin, F. Ducros, D. Veynante, T. Poinsot, A thickened flame model for large eddy simulations of turbulent premixed combustion, Phys. Fluids 12 (7) (2000) 1843–1863.
[184] F. Charlette, C. Meneveau, D. Veynante, A power-law flame wrinkling model for LES of premixed turbulent combustion part II: dynamic formulation, Combust. Flame 131 (1–2) (2002) 181–197.
[185] D. Veynante, V. Moureau, Analysis of dynamic models for large eddy simulations of turbulent premixed combustion, Combust. Flame 162 (12) (2015) 4622–4642.
[186] H. Kolla, J.W. Rogerson, N. Chakraborty, N. Swaminathan, Scalar dissipation rate modeling and its validation, Combust. Sci. Technol. 181 (3) (2009) 518–535.
[187] G. Lecocq, S. Richard, O. Colin, L. Vervisch, Hybrid presumed pdf and flame surface density approaches for large-eddy simulation of premixed turbulent combustion. part 1: formalism and simulation of a quasi-steady burner, Combust. Flame 158 (6) (2011) 1201–1214.
[188] J.B. Bell, M.S. Day, I.G. Shepherd, M.R. Johnson, R.K. Cheng, J.F. Grcar, V.E. Beckner, M.J. Lijewski, Numerical simulation of a laboratory-scale turbulent V-flame, Proc. National Academy of Sciences 102 (29) (2005) 10006–10011.
[189] H. Wang, E.R. Hawkes, J.H. Chen, B. Zhou, Z. Li, M. Aldén, Direct numerical simulations of a high Karlovitz number laboratory premixed jet flame–an analysis of flame stretch and flame thickening, J. Fluid Mech. 815 (2017) 511–536.
[190] N. Chakraborty, R. Cant, Effects of lewis number on flame surface density transport in turbulent premixed combustion, Combust. Flame 158 (9) (2011) 1768–1787.
[191] P.E. Lapenna, L. Berger, A. Attili, R. Lamioni, N. Fogla, H. Pitsch, F. Creta, Data-driven subfilter modelling of thermo-diffusively unstable hydrogen–air premixed flames, Combust. Theor. Model. 25 (6) (2021) 1064–1085.
[192] D. Haworth, Numerical simulations of Lewis number effects in turbulent premixed flames, J. Fluid Mech. 244 (1992) 405–436.
[193] C. Rutland, A. Trouvé, Direct simulations of premixed turbulent flames with nonunity Lewis numbers, Combust. Flame 94 (1–2) (1993) 41–57.
[194] N. Chakraborty, R.S. Cant, Effects of Lewis number on scalar transport in turbulent premixed flames, Phys. Fluids 21 (3) (2009) 035110.
[195] N. Chakraborty, R. Cant, Effects of Lewis number on turbulent scalar transport and its modelling in turbulent premixed flames, Combust. Flame 156 (7) (2009) 1427–1444.
[196] R. Rasool, N. Chakraborty, M. Klein, Effect of non-ambient pressure conditions and lewis number variation on direct numerical simulation of turbulent Bunsen flames at low turbulence intensity, Combust. Flame 231 (2021) 111500.
[197] T. Dunstan, N. Swaminathan, K. Bray, N. Kingsbury, The effects of non-unity Lewis numbers on turbulent premixed flame interactions in a twin V-flame configuration, Combust. Sci. Technol. 185 (6) (2013) 874–897.
[198] B. Savard, G. Blanquart, Broken reaction zone and differential diffusion effects in high Karlovitz n-C7H16 premixed turbulent flames, Combust. Flame 162 (5) (2015) 2020–2033.
[199] A.J. Aspden, M.S. Day, J.B. Bell, Towards the distributed burning regime in turbulent premixed flames, J. Fluid Mech. 871 (2019) 1–21.
[200] A. Aspden, J. Bell, M. Day, F. Egolfopoulos, Turbulence-flame interactions in lean premixed dodecane flames, Proc. Combust. Inst. 36 (2) (2017) 2005–2016.
[201] H. Lee, P. Dai, M. Wan, A. Lipatnikov, Influence of molecular transport on burning rate and conditioned species concentrations in highly turbulent premixed flames, J. Fluid Mech. 928 (2021).
[202] H. Lee, P. Dai, M. Wan, A. Lipatnikov, A dns study of extreme and leading points in lean hydro-

Please cite this article as: S. Hochgreb, How fast can we burn, 2.0, Proceedings of the Combustion Institute, https://doi.org/10.1016/j.proci.2022.06.029

gen-air turbulent flames–part I: local thermochemical structure and reaction rates, Combust. Flame (2021).
[203] S. Lapointe, B. Savard, G. Blanquart, Differential diffusion effects, distributed burning, and local extinctions in high Karlovitz premixed flames, Combust. Flame 162 (9) (2015) 3341–3355.
[204] S. Lapointe, G. Blanquart, Fuel and chemistry effects in high Karlovitz premixed turbulent flames, Combust. Flame 167 (2016) 294–307.
[205] E. Suillaud, K. Truffin, O. Colin, D. Veynante, Direct numerical simulations of high Karlovitz number premixed flames for the analysis and modeling of the displacement speed, Combust. Flame 236 (2022).
[206] L. Berger, A. Attili, H. Pitsch, Intrinsic instabilities in premixed hydrogen flames: parametric variation of pressure, equivalence ratio, and temperature. part 1 - dispersion relations in the linear regime, Combust. Flame (2022) 111935.
[207] T. Howarth, A. Aspden, An empirical characteristic scaling model for freely-propagating lean premixed hydrogen flames, Combust. Flame 237 (2022).

Please cite this article as: S. Hochgreb, How fast can we burn, 2.0, Proceedings of the Combustion Institute, https://doi.org/10.1016/j.proci.2022.06.029